



## Using the International Tree-Ring Data Bank (ITRDB) records as century-long benchmarks for land-surface models

Jina Jeong<sup>1</sup>, Jonathan Barichivich<sup>2,3</sup>, Philippe Peylin<sup>2</sup>, Vanessa Haverd<sup>4</sup>, Matthew J. McGrath<sup>2</sup>, Nicolas Vuichard<sup>2</sup>, Michael N. Evans<sup>5</sup>, Flurin Babst<sup>6,7,8</sup> and Sebastiaan Luyssaert<sup>1</sup>

- 5 <sup>1</sup> Department of Ecological Sciences, VU University, 1081HV Amsterdam, the Netherlands.  
<sup>2</sup> Laboratoire des Sciences du Climat et de l'Environnement, IPSL, CNRS/CEA/UVSQ, 91191 Gif sur Yvette, France.  
<sup>3</sup> Instituto de Conservación Biodiversidad y Territorio, Universidad Austral de Chile, 5090000 Valdivia, Chile.  
<sup>4</sup> CSIRO Oceans and Atmosphere, Canberra, 2601, Australia.  
<sup>5</sup> Department of Geology & ESSIC, University of Maryland, MD 20742-4211, USA.  
10 <sup>6</sup> Dendro Sciences Group, Swiss Federal Research Institute WSL, Zürcherstrasse 111, CH-8903 Birmensdorf  
<sup>7</sup> School of Natural Resources and the Environment, University of Arizona, Tucson, USA  
<sup>8</sup> Laboratory of Tree-Ring Research, University of Arizona, Tucson, USA

**Running head:** Tree-ring records as century-long benchmarks

15

*Correspondence to:* Jina Jeong ([j.jeong@vu.nl](mailto:j.jeong@vu.nl))

**Key words:** forest growth, tree-ring width, diameter growth, climate sensitivity, size-dependent growth, climate change



## Abstract

20 The search for a long-term benchmark for land-surface models (LSM) has brought tree-ring data to the attention of the land-surface community as they record growth well before human-induced environmental changes became important. The most comprehensive archive of publicly shared tree-ring data is the International Tree-ring Data Bank (ITRDB). Many records in the ITRDB have, however, been collected almost exclusively with a view on maximizing an environmental target signal (e.g. climate), which has resulted in a biased representation of forested sites and landscapes and thus limits its use as a data source

25 for benchmarking. The aim of this study is to propose advances in land-surface modelling and data processing to enable the land-surface community to re-use the ITRDB data as a much-needed century-long benchmark. Given that tree-ring width is largely explained by phenology, tree size, and climate sensitivity, LSMs that intend to use it as a benchmark should at least simulate tree phenology, size-dependent growth, differently-sized trees within a stand, and responses to changes in temperature, precipitation and atmospheric CO<sub>2</sub> concentrations. Yet, even if LSMs were capable of accurately simulating tree-

30 ring width, sampling biases in the ITRDB need to be accounted for. This study proposes two solutions: exploiting the observation that the variation due to size-related growth by far exceeds the variation due to environmental changes; and simulating a size-structured population of trees. Combining the proposed advances in modelling and data processing resulted in four complementary benchmarks - reflecting different usage of the information contained in the ITRDB - each described by two metrics rooted in statistics that quantify the performance of the benchmark. Although the proposed benchmarks are

35 unlikely to be precise, they advance the field by providing a much-needed large-scale constraint on changes in the simulated maximum tree diameter and annual growth increment for the transition from pre-industrial to present-day environmental conditions over the past century. Hence, the proposed benchmarks open up new ways of exploring the ITRDB archive, stimulate the dendrochronological community to refine its sampling protocols to produce new and spatially unbiased tree-ring networks, and help the modelling community to move beyond the short-term benchmarking of LSM.

40

## 1. Introduction



Earth system models integrate numerical models of atmospheric circulation, ocean dynamics and biogeochemistry, sea ice dynamics, and biophysical and biogeochemical processes at the land-surface. Climate projections made by Earth system models have been the corner-stone of the last five Assessment Reports of the Intergovernmental Panel on Climate Change (IPCC, 2013) and as such have made a tremendous impact on global environmental policy (Hecht and Tirpak, 1995). The credibility of projections of the future climate from any Earth system model hinges on the ability of each of the four model components of an Earth system model to accurately reproduce the past (McGuffie, 2005). Although long-term changes that dates back to pre-industrial conditions (Luo et al., 2012) have been documented for vegetation distribution through pollen based reconstructions (Cao et al., 2019), land-surface models currently lack a long-term benchmark for ecosystem functioning. The absence of long-term benchmarks is thought to contribute substantial uncertainty to future global carbon stocks in soil and vegetation (Friedlingstein et al., 2006; Friedlingstein et al., 2014) and as such to climate projections (Fig. 1a).

Tree-ring records provide annual information on historical tree growth and physiology in relation to environmental conditions including the era before human activities started to affect the atmospheric CO<sub>2</sub> concentration (Fritts, 2012; Hemming et al., 2001). Even though trees grown in the absence of climatic stress may not develop distinct tree-rings as has been observed for several species from the humid tropics, hence, tree-ring records have been proposed as a large-scale long-term benchmark for the land surface component of Earth system models (Fig. 1b) (Babst et al., 2014a, 2014b, 2017, 2018; Zuidema et al., 2018).

Until now tree-ring records have been collected almost exclusively to reconstruct past climate and hydrological variability from sites where trees grow near the colder or drier fringes of their distribution (Briffa et al., 2004; D'Arrigo et al., 2008). The most comprehensive archive of publicly shared tree-ring data is the International Tree-ring Data Bank (ITRDB), with more than 4,000 locations from 226 species across most forested biomes (Grissino-Mayer and Fritts, 1997; Zhao et al., 2019). However, a shortage of site metadata and the prevailing geographical, species and tree selection sampling biases resulting from targeting climate-sensitive trees has limited the use of the ITRDB archive to infer long-term changes in forest growth (Bowman et al., 2013; Briffa and Melvin, 2011; Klesse et al., 2018; Zhao et al., 2019). These issues may, likewise, limit the information content of the ITRDB records compared to tree ring records that were collected for the purpose of benchmarking land-surface



models (<http://www.baci-h2020.eu/>). This loss in information content should, however, be balanced against the associated benefits of re-using data in terms of time gain and resource savings.

70

When tree rings are to be used as benchmarks for land surface models, the models will need the skill to mechanistically simulate tree-ring width (TRW). In the past decades, the major physiological and ecological processes that are responsible for annual tree-ring growth became sufficiently well-understood to be formalized in mathematical models with different levels of details and complexities. The first TRW models (Wilson and Howard, 1968) described processes at the cell level: cell division, cell enlargement, and cell wall thickening. Later, the carbon and water balance of trees was added (Fritts et al., 1999) as well as climatic influences on cambial activity (Vaganov et al., 2006). These models were capable of reproducing short-term radial growth at the tree level. Further developments introduced a notion of turgor and hormone regulation for cell growth (Drew et al., 2010; Hölttä et al., 2006; De Schepper and Steppe, 2010; Steppe et al., 2006).

75

80

At the same time, the spatial scale of models simulating wood formation based on cell dynamics was extended to the stand level by simplifying process representation. In one such model, photosynthate availability, air temperature and soil water content were used to constrain wood cell growth and successfully reproduced observations (Deleuze and Houllier, 1998; Hayat et al., 2017; Wilkinson et al., 2015). Further simplifications were proposed by simulating the radial growth of trees based solely on carbon allocation (Deleuze et al., 2004; Merganičová et al., 2019) rather than cell dynamics, the latter being computationally too expensive for large scale vegetation models (Li et al., 2014; Misson et al., 2004; Sato et al., 2007). Hence, a variety of approaches are now available to describe TRW growth in forest models, dynamic vegetation models and land-surface models, but to the best of our knowledge there is yet no land surface component of an Earth system model with such capability.

85

90

This study articulates an improved conceptual framework for benchmarking simulated radial growth against ITRDB tree-ring data, addressing limitations in the models, the data and the methods to compare models and data. The aims are to: (1) use current understanding of tree-ring growth to derive the minimal requirements for benchmarking land-surface models against



tree-ring records archived in the ITRDB; (2) review potential issues of using the ITRDB to benchmark land-surface models; (3) propose solutions for a meaningful comparison of land-surface models against ITRDB records; and (4) demonstrate the proposed methodological framework by benchmarking a land-surface model across ten European Scots pine (*Pinus sylvestris* L.) forests using tree-ring width chronologies archived in the ITRDB.

## 2. Background: model requirements and data limitations

### 2.1. Minimal requirements for land-surface models to mechanistically simulate TRW

The aggregate tree growth model (Cook and Kairiukstis, 1990) considers that the observed TRW at year  $t$  (in mm) consists of additive growth contributions (Fig. 2):

(i) Size-dependent growth is the dominant signal in tree-ring records (Cook et al., 1995). Conceptually it can be understood by considering an almost constant volume of wood due to a more or less constant primary production (Hirata et al., 2007) being added to the trunks year after year (Nash, 2011). The annual diameter increment of the trees will decrease as the trunk grows because a given wood volume has to be distributed over an increasing surface area as both the circumference and height of the stem are increasing. In reality, however, self-thinning reduces stand density and competition for resources, implying that the remaining trees can increase their crown volume and thus increase their primary production (Oliver and Larson, 1996) which largely compensates for the size-dependent decrease in TRW and contributes to the observed almost constant TRW of tall trees. Several of the common allocation schemes used in land-surface models account for size-dependent growth and self-thinning (Franklin et al., 2012; Wolf et al., 2011).

(ii) Climate-dependent growth reflects the sensitivity of tree growth to radiation, temperature, and water availability (Fritts, 2012) and is well-developed in land-surface models, as it represents the core purpose of this type of model. Land-surface models often rely on the Farquhar model for the radiation and temperature dependency of photosynthesis (Farquhar, 1989), the McCree - de Wit - Penning de Vries - Thornley approach for the temperature dependence of respiration (Amthor,



2000), and account for a decoupling of photosynthesis and growth by the use of a labile carbon pool (Friend et al., 2019; Naudts et al., 2015; Zaehle and Friend, 2010). Plant water availability is accounted for through either simple transfer functions or more recently by accounting for the hydraulic architecture of the simulated trees (Bonan et al., 2014; Naudts et al., 2015).

(iii) Endogenous disturbances refer to within-stand resource competition and are being increasingly simulated in land-surface models albeit often by empirical approaches (Haverd et al., 2013; Moorcroft et al., 2001; Naudts et al., 2015). From a benchmarking point of view, simulating individuals of different size or cohorts within a single forest is essential to reproduce the sampling biases present in the ITRDB (see section 3 below). Chronic exogenous disturbances such as increasing atmospheric CO<sub>2</sub> concentration (LaMarche et al., 1984) and N-deposition (Magnani et al., 2007) are also well-developed as they are among the main purposes of using land-surface models. The effect of CO<sub>2</sub> fertilization on photosynthesis is accounted for in the photosynthetic submodel (see above) whereas nitrogen dynamics are accounted for through static or dynamic stoichiometric approaches (Vuichard et al., 2019; Zaehle and Friend, 2010).

(iv) Although abrupt disturbances such as fires, pests and storms are increasingly being simulated by land-surface models (Chen et al., 2018; Yue et al., 2014) these functionalities are at present of limited use for benchmarking against TRW data. Abrupt disturbances are often simulated as stand-replacing disturbances and will, therefore, not be reflected in the simulated TRWs. Furthermore, the timing of such events largely depends on the simulated diagnostics, for example, fuel wood build-up, insect population dynamics, and soil moisture, which could strongly deviate from the observed timing in decadal to century long simulation periods.

(v) The final term in the aggregate tree growth model constitutes all processes and interactions between processes not previously accounted for in the land-surface model, and will make up the model error.

This aggregate tree growth model provides the conceptual basis for tree-ring standardization and climate signal extraction methods used in dendrochronology (Briffa and Melvin, 2011; Cook and Kairiukstis, 1990), which rely on the assumptions that the sampled trees capture the relevant growth variability of the stand and that the contribution of each major driver can be



statistically identified as either signal or noise. If tree-rings are formed, observed TRW records cannot, however, be fully decomposed in the absence of metadata because several drivers do not leave a unique fingerprint in the tree-ring record.  
45 However, size effect and climate sensitivity have a much larger contribution to TRW than the other processes (Hughes et al., 2011). Nevertheless, alternative approaches have been proposed to attribute TRW to its major drivers (Stine, 2019).

In addition to accurate process representation, the model will need to be driven by historical climate, atmospheric CO<sub>2</sub> concentrations and N-deposition. In general, commonly-used century-long climate reanalyses such as NCEP (Kalnay et al., 1996),  
50 20CR (Compo et al., 2011), and CERA-20C (Laloyaux et al., 2018) are based on the assimilation of instrumental observations in climate simulations and are thus independent from tree-ring-based observations or other proxy data. Nevertheless, the accuracy of the reanalyses decreases proportional to data availability, particularly in remote areas with a low density and temporal depth of meteorological stations, and given that local climate effects may have contributed to the TRW, it might be desirable to align the reanalysis with present day site-specific observations where they exist (Ols et al., 2018). When LSMs  
55 are forced by actual climate observations, reproducing the observed climate sensitivity in tree rings would both facilitate and add credibility to the land-surface simulation – if forcing, LSM and TRW models are all realistic and unbiased.

Given the above, land-surface models that intend to use TRWs as a benchmark should at the minimum simulate: (1) dynamic plant phenology, (2) size-dependent growth, (3) differently-sized trees within a stand, and (4) responses to chronic exogenous  
60 environmental changes (Fig. 2). Whereas responses to chronic exogenous environmental changes are the reason LSMs exist and are therefore to some extent accounted for by all current LSMs, size-dependent growth and size differentiation within a stand are at present only accounted for in few land surface models, for example, CLM (ED) (Fisher et al., 2015), ORCHIDEE (Naudts et al., 2015), and LPJ-GUESS (Smith, 2001). Revision 5698 of the ORCHIDEE model meets the aforementioned minimum requirements and therefore will be used in this study.

65

## 2.2. Challenges of using ITRDB data as a long-term benchmark



70 A typical record in the ITRDB consists of TRW measurement of increment cores from tens of individual trees from the same site and species. Each record may have a different starting date, ending date and thus length (Fig. 3 a and b). If a core reaches the centre of the trunk, annual tree diameter can be reconstructed (Bakker, 2005). Even then diameter reconstruction may come with some uncertainty because trunks are not perfectly round. If the core does not contain the centre of the trunk, which is often the case for large trees, rings near the pith will be missed adding uncertainty to the diameter and age reconstruction (Briffa and Melvin, 2011).

75 Despite of known biases in the ITRDB, it can be used to extract information useful for LSMs. The predominant sampling design in the ITRDB targets the presumably oldest trees, which should give the longest time series and are therefore be most useful to reconstruct the climate variability prior to instrumental records. The ITRDB is thus likely to overrepresent large trees (Brienen et al., 2012; Nehrbass-Ahles et al., 2014) relative to the population demographics at time of sampling. This big-tree bias makes the ITRDB unsuitable to upscale growth of individual trees to larger spatial domains, i.e., stand, forest or the region (Babst et al., 2014a; Nehrbass-Ahles et al., 2014) but does not affect the value of the ITRDB archive for documenting individual tree growth as long as tree size and dominance effects are explicitly considered. Although the model-data comparison cannot -without additional data- correct for the big-tree bias in the ITRDB, models that simulate multiple tree diameter classes may accommodate this bias by comparing the largest simulated diameter class with the observed ITRDB tree-ring records (Fig. 3a).

85 Another bias related to the ITRDB sampling design comes from the fact that the growth rate of trees within a cohort differs between individuals (Melvin, 2004; Zuidema et al., 2011) resulting in slowly and fast-growing trees within the same cohort (Fig. 3b). Slow-growing trees tend to live longer than fast-growing trees in the same cohort (Mencuccini et al., 2005; Schulman, 1954). Records of TRW are thus likely to underestimate the mean tree growth of a stand in long-passed centuries as fast-growing trees would have died off before the samples were taken (Brienen et al., 2012).

90





The other challenge of using ITRDB data is rooted in the difference between the observed and simulated forest structure. Tree-ring datasets are composed by cores of individuals from different cohorts (Fig. 3b). Comparing these data against simulations requires the model to be individual based or to align TRW records by age (Fig. 3a).

95

Given the above, only part of the information contained in TRW records can be used for benchmarking if their sampling protocol is poorly described or not rigorously enforced. A model-data comparison cannot correct for these biases but consistency between modelled and observed tree-rings for a stand under study can be improved by making use of virtual trees. As the output of LSMs must be coupled to realistic models for TRW, careful post-processing of the ITRDB data may be required to become suitable benchmarks for land surface models. The proposed benchmarks, thus, use three different

100

definitions of virtual trees each of which addresses different aspects:

(1) the average virtual tree of a stand aligned by tree age is calculated as the time series for the average ring width after aligning the age of the individual trees (Fig. 3a). Age-aligned tree-ring widths are widely used to calculate a statistic known as the mean regional curve of the sampled stand (Briffa and Melvin, 2011). This assumes that common drivers regardless of time, exceed

105

the signal from local and individual differences in tree growth (see subsection 4.2 (i));

(2) the average virtual tree of a stand aligned by calendar year is calculated by ordering individual tree records by calendar year (Fig. 3b) and for each year the average observed diameter is calculated. Alignment by calendar year thus reflects the real temporal evolution of the stand. This virtual tree can be used to cope with the challenge from difference in forest structure between the simulation and the observation by compiling a representative and comparable tree with the simulated tree (see

110

subsection 4.2 (ii));

(3) the largest virtual tree of a stand is calculated after aligning individual trees by their age (Fig. 3c). The recommendation to remove the age trend from tree-ring records (Cook et al., 1995) confirms the assumption underling the alignment by age, i.e., that size dependent age exceeds the growth trends due to long-term environmental changes. Subsequently, the age-aligned TRWs can be used to compile a virtual fast-growing tree which has the maximum observed diameter of all trees for a given

115

(iii)).



The proposed data-model comparison thus relies on the concept of virtual trees to account for known sampling biases of the ITRDB as well as for the model definition of a forest stand. The validity of the concept of a virtual tree is evaluated in section 4.1. Except for land surface models with an individual tree-based stand definition (Sato et al., 2007), benchmarking other models will have to consider the use of virtual trees as well. Hence, the proposed definitions and uses of virtual trees are specific to ORCHIDEE r5698.

### 3. Materials and Methods

#### 3.1. The land-surface model ORCHIDEE

ORCHIDEE (Ducoudré et al., 1993; Krinner et al., 2005) is the land-surface model of the IPSL (Institute Pierre Simon Laplace) Earth system model (Dufrêne et al., 2005). Hence, by design, it can be coupled to an atmospheric general global circulation model or become a component in a fully coupled Earth system model. In a coupled setup, the atmospheric conditions affect the land-surface and the land-surface, in turn, affects the atmospheric conditions. However, when a study focuses on changes in the land-surface rather than on the interactions with climate, it can also be run as a stand-alone land-surface model. In both configurations the model receives as input atmospheric conditions such as precipitation, air temperature, air humidity, and incoming solar radiation, and CO<sub>2</sub>; this combination of inputs is known as the climate forcing. Both configurations can cover any area ranging from global to regional domains and even down to a single grid point for the stand-alone case.

Although ORCHIDEE does not enforce a spatial or temporal resolution, the model does use a predefined spatial grid and equidistant time steps. The spatial resolution is an implicit user setting that is determined by the resolution of the climate forcing. Although the temporal resolution is not fixed, the processes were formalized at given time step: half-hourly (i.e. photosynthesis and energy budget), daily (i.e. net primary production), and annually (i.e. vegetation dynamics). Hence, meaningful simulations have a temporal resolution between 1 minute and 1 hour for the energy balance, water balance, and photosynthesis calculations.



ORCHIDEE builds on the concept of meta-classes to describe vegetation distribution. By default, it distinguishes 13 meta-classes (one for bare soil, eight for forests, two for grasslands, and two for croplands). Each meta-class can be subdivided into an unlimited number of plant functional types (PFTs). When simulations make use of species-specific parameters and age classes, several PFTs belonging to a single meta-class will be defined. Biogeochemical and biophysical variables are calculated for each PFT or groups of PFTs (e.g. all tree PFTs in a pixel drawn from the same description of soil hydrology, known as a soil water column).

ORCHIDEE is not an individual-based model but instead represents forest stand complexity and stand dynamics with diameter and age classes. Each class contains a number of individuals that represent the mean state of the class. Therefore, each diameter class contains a single modelled tree that is replicated multiple times and distributed at random throughout the PFT area. At the start of a simulation, each PFT contains a user-defined number of stem diameter classes. This number is held constant throughout the simulation, whereas the diameter boundaries of the classes are adjusted to accommodate for temporal evolution in the stand structure. By using flexible class boundaries with a fixed number of diameter classes, different forest structures can be simulated. An even-aged forest, for example, is simulated with a small diameter range between the smallest and largest classes. All classes will then effectively belong to the same stratum. An uneven-aged forest is simulated by applying a large range between the diameter classes. Different diameter classes will therefore effectively represent different strata. The limitations of this approach become apparent when the tree-ring width data and simulation are compared by calendar year as the model does not track individual trees. Although the model tree itself is well-defined, the amount of radiation it receives (and therefore the amount of carbon produced) is determined by the statistical distribution of all model trees in that grid cell.

Vegetation structure is then used for the calculation of the biophysical and biogeochemical processes of the model such as photosynthesis, plant hydraulic stress, and radiative transfer model. The r5698 version of ORCHIDEE, which is the version used in this study, combines the dynamic nitrogen cycle of ORCHIDEE r4999 (Vuichard et al., 2019; Zaehle and Friend, 2010) and the explicit canopy representation of ORCHIDEE r4262 (Chen et al., 2016; Naudts et al., 2015; Ryder et al., 2016). It is one of the branches of the ORCHIDEE model and it was further developed from Naudts et al. (2015) and Vuichard et al.



(2019) (Text S1), parameterized, and tested to simulate tree-ring widths, in order to meet the aforementioned minimum requirements of simulating the carbon, water, energy, and nitrogen cycle, while accounting for size-dependent allocation for three diameter classes within a forest stand.

70

In this study we use a climate data product from a merged and homogenized gridded dataset developed for modelling purpose over the 20<sup>th</sup> century, i.e., CRU-NCEP (Viovy, 2016), such that observed tree-ring widths for the past century can be used to evaluate the skill of the land-surface model ORCHIDEE r5698 to simulate radial tree growth. A detailed overview of earlier developments (Krinner et al., 2005; Naudts et al., 2015; Vuichard et al., 2019) that resulted in the emerging capability of ORCHIDEE r5698 to match the aggregate tree growth model (Fig. 2) is given in the supplementary material (Text S1).

75

### 3.2. Simulation set-up for the data-model comparison

We selected 10 forest sites from the ITRDB for comparison with simulations, based on the following criteria: (1) located in Europe; (2) composed of *Pinus sylvestris* L.; (3) between 100 to 150 years old; and (4) ranging from Spain to Finland and therefore thought to largely cover the climatic conditions encountered across the species range of *P. sylvestris* within Europe. The location of the selected forests is detailed in Table S2. ORCHIDEE r5698 was run for 10 individual pixels, each containing one of the selected sites. An observed time series of atmospheric CO<sub>2</sub> concentrations was used (Keeling et al., 1996) and all forest were considered to be unmanaged. Every simulation started from a 300-year long spinup required to bring the simulation to equilibrium with respect to the slow carbon and nitrogen pools in the soil. The start year and the length of each simulation was set to match the site observations. A more detailed description of the test case and the ORCHIDEE model is given in the Supplementary Information (Text S2).

80

85

The model run was repeated four times for every site to obtain simulated tree ring widths for four different model configurations. The first configuration is the most basic configuration in this test (hence its label 'basic'): sapling recruitment is not accounted for, the nitrogen cycle is open and the parameter quantifying resource competition within a stand ( $f_{\text{power}}$ , for more details see Text S1 Eq. 15 and 16) was fixed at 2. The second configuration (labelled 'power') was a copy of the first

90



but used a modified expression for resource competition (Eq. 16 in Supplementary Information) was used ('power'). The third configuration built on the second but also accounted for recruitment ('recru'). Finally, the fourth configuration used a closed and dynamic nitrogen cycle, recruitment, and the modified within-stand competition  $f_{\text{power}}$  ('Ndyn').

.95

The configuration with an open nitrogen cycle prescribed the leaf carbon-to-nitrogen-ratios with the average leaf carbon-to-nitrogen-ratio obtained from the 'Ndyn' simulation following the method proposed by Vuichard et al. (2019). This ensured that the differences came from the C-N feedbacks rather than from differences in leaf nitrogen. In the absence of bias corrected climate forcing, the simulations cycled through the climate forcing from 1901 to 1910 for the years prior to 1901. From 1901 onwards, climate forcing matching the simulation years was used. The four configurations with increasing model functionality are summarized in Table 2.

.00

### 3.3. Reference data of ecologically sampled TRW data

A "fixed-plot approach" TRW database was established under the BACI project (<http://www.baci-h2020.eu/>) by archiving 48 datasets from multiple research efforts in Europe (Klesse et al., 2018). To be retained and archived, *all* trees larger than 5.6 cm in diameter had to be sampled in a 10 to 40 m radius plot of which the exact radius depended on stand density (Babst et al., 2014). The BACI archive is, therefore, considered to be free from the big-tree selection bias which is present in the ITRDB. The records from BACI were used to evaluate the validity of using virtual trees constructed from ITRDB records to combat the aforementioned sampling biases.

.05

.10

For all four benchmarks each reflecting a different usage of the information contained in the ITRDB, the virtual trees were constructed by making use of only the top 15% of the trees based on their diameter. The 15% threshold was taken to match the diameter distribution in ORCHIDEE where by definition the largest diameter class contains 15% of the trees. Subsequently, the ratio of the diameter of the virtual trees over the diameter of the average stand diameter was calculated to estimate the error introduced by using a virtual tree. Only the 27 coniferous forests contained in the BACI archive were selected to enhance consistency within our test case.

.15



## 4. Results

### 4.1. Evaluating the concept of virtual trees

20 The bias introduced by constructing a virtual tree based on the diameters of the largest 15% of the trees from the  
representatively-sampled BACI data sets is thought to be a proxy of the bias inherent to the ITRDB (Fig. 4). No statistically  
significant differences were found between the simulation-based and data-based virtual trees except for the virtual tree used in  
the benchmark for young trees (t-test,  $p < 0.01$ ). In the latter case the statistical difference seems to be caused the lack of  
25 of variation in the simulation-based tree rather than a large difference between the means of the virtual trees (Fig. 4). This lack  
of variation for the simulation-based tree is expected as the method uses the maximum simulated diameter. Hence, the test  
supports the use of virtual trees constructed from the ITRDB as a benchmark for the largest diameter class of a forest simulated  
by ORCHIDEE.

### 4.2. Benchmarks for comparing observed and simulated tree-ring widths

30 If a land-surface model explicitly accounts for the main factors contributing to TRW, i.e., size effects and climate sensitivity  
(Hughes et al., 2011), meaningful benchmarking against specific aspects of the observations becomes feasible in spite of the  
aforementioned biases in the ITRDB. Our technical framework considers four complementary aspects of the observations: (i)  
the size-related trend in tree-rings; (ii) diameter increment of mature trees; (iii) diameter increment of young trees; and (iv)  
extreme growth events. Each of these aspects formed the basis of a benchmark (Table 1):

35  
(i) The size-related trend in diameter increment can be assessed by calculating the average virtual tree for a stand aligned  
by tree age (Fig. 5 a, b) and subtracting its TRWs from the simulated TRWs of the largest diameter class (Fig. 5c).  
Subsequently, a linear regression is used to quantify the temporal trend in the residuals (Fig. 5d). If the simulations and  
observations have similar size-related trends, the temporal trend in the residuals will be close to zero. Furthermore, the root  
40 mean square error (RMSE) between the simulations and observations is calculated and normalized by the length of time series



used to calculate the difference in observed and simulated growth trends. A skilled model is expected to simultaneously show no trend in the residuals and a low RMSE across many sites.

(ii) Diameter increments of mature trees. In land-surface models that account for within-stand competition, larger trees will consistently grow faster than smaller trees due to the way competition is formalized (Bellassen et al., 2010; Haverd et al., 2013). In reality, growing conditions can suddenly become favourable for trees that have previously been suppressed, resulting in fluctuating growth rates. This discrepancy between simulated and observed competition can be accounted for in the benchmark by using the observations to compile a virtual tree of the stand aligned by calendar year, taking the average tree diameter of all samples to construct the virtual tree (Fig. 6 a and b). Under the assumption that the observed trees are the biggest trees from a given site, the virtual tree can be compared with the biggest diameter class from the model (see section 4.1). Given that for the last decades both the quick and slowly growing trees are still alive and could have been sampled, only the growth in recent decades of the virtual tree are compared to the simulations (Fig. 6 c and d). The RMSE and trend of the residuals between the virtual tree and the largest diameter class simulated are calculated (Fig. 6d). A skilled model is expected to simultaneously show no trend in the residuals and a low RMSE across many sites.

(iii) Diameter increments of young trees. As mentioned above, the size-related trend in diameter increment can be assessed by calculating the largest virtual tree of the stand. The maximum age of a virtual tree equals the shortest observed individual TRW record for the stand, as it represents the age intersection between the TRW records for all individuals in the stand. The largest virtual tree is thus clearly biased towards higher observed diameters, compensating for the loss of observed high diameters in the sampling approach due to the fact that the old fast-growing trees died well before sampling took place (Fig. 7 a and b). The first decades of growth of the virtual tree are then compared to the simulated growth of the largest diameter class (Fig. 7 c and d) by calculating the RMSE and trend of the residuals (Fig. 7d). A skilled model is expected to simultaneously show no trend in the residuals and a low RMSE across many sites. By using different approaches to evaluate the growth of young (this benchmark) and mature trees (the previous benchmark) the comparison accounts for the observation that the drivers of ring growth change when the trees grow taller (Cook, 1985).



(iv) Extreme growth events. Even a perfect land-surface model cannot be expected to reproduce all year-to-year variation due to uncertainties in forcing data, such as the reconstructed climate and N-deposition drivers. Nevertheless, well-constrained climate reconstructions can be expected to contain extreme events, and hence a skilled model driven by well-constrained reconstructions should reproduce the statistics of the most extreme events. In this benchmark, extreme growth is defined as the first and last quartiles in TRW ordered by calendar year (i.e., not aligning establishment years) and averaged over the individual trees records (Fig. 8a). The model skill to reproduce the absolute ring-width amplitude regardless of timing was tested by comparing the observed and simulated 25th and 75th percentiles of TRWs for the largest diameter class, which is the diameter class showing the strongest climate sensitivity (Fig. 8 e and f). Additionally, model skill for reproducing the timing of individual extreme growth events was tested by comparing the simulated TRW for the exact years during which extreme growth was observed (Rammig et al., 2015; Fig.8 a-d). For both the amplitude and timing of growth extremes, the similarity between simulations and observations was calculated as the RMSE with the error being the distance from the 1:1 line (Fig. 8 c-f). A skilled model is expected to simultaneously show low RMSE for both the amplitude and timing of extreme years across many sites.

80

### 4.3. Test case

As the test case aimed at illustrating the four benchmarks rather than evaluating the ORCHIDEE model itself, the main objective of the test case is confirming that each benchmark indeed tests different aspects of the model's performance and that the proposed benchmarks can, therefore, be considered complementary to each other. The four benchmarks presented above were applied to a test case consisting of ten *Pinus sylvestris* L. sites across Europe. For each site the dataset consisted of 11 to 304 cores (Table S2); a leave-one-out approach was used to evaluate the sensitivity of the benchmark to individual tree records. For the simulations, the land-surface model ORCHIDEE r5698 was used. This model versions accounts for the aforementioned minimum requirements for land surface models to mechanistically simulate TRW. The benchmarks were used on four configurations with increasing model functionality (Table 2). A more detailed description of the test case, the ORCHIDEE model and the different configurations is given in the Supplementary Information (Text S1 and S2).

90





The model reproduced the observed age-trends across the four configurations tested, i.e., the ‘basic’ set-up, the ‘recru’ set-up with an increasing number of individuals through recruitment (Eqs. 28 and 29 in Text S1), the ‘power’ set-up with a decreasing share of stand-level photosynthesis allocated to the largest size classes (Eq. 15 in Text S1), and the ‘Ndyn’ set-up where growth may be limited by additional nitrogen requirements (Eq. 32 in Text S1). Increasing the functionality of the model did not help to reduce the RMSE of the overall age trend but did improve the match (i.e. the slope) between the simulated and observed age trends at 8 of 10 sites (Fig. 9a). For mature trees, the additional functionality acted as an offset, and hence growth rate estimates of the largest trees containing the biggest share of stand biomass improved at sites where diameter growth was underestimated (indicated by the trend in the residuals). Diameter growth rates were, however, further overestimated at sites where this was already the case (Fig. 9b). The RMSE of the diameter of mature trees (Fig. 9b, x-axis) were negatively correlated with their growth rate (Fig. 9b, y-axis) ( $\rho = -0.5$ ,  $p < 0.01$ ), suggesting that little new insight is to be expected from using both metrics from this benchmarks (Table 1) compared to simply selecting one.

Increasing model functionality had a much smaller effect on early stand developmental stages, as shown by the much smaller absolute changes in both RMSE and trends in the residuals for the young trees (Fig. 9c) compared to the old trees (Fig. 9b). Interestingly, considering feedbacks between the nitrogen and carbon cycles (configuration ‘Ndyn’) increased the RSME for forests located in regions with relatively low nitrogen deposition loads (Fig 9c, x-axis). When the dynamic nitrogen cycle is used, the carbon-to-nitrogen ratio in the leaves increases with increasing age whereas it remains constant for the open nitrogen cycle used in the other three configurations. This simulated age-related dynamic for leaf nitrogen in combination with its initial value contributes to the overestimation of the TRW for young trees. Finally, adding functionality to the model did not help to enhance the model skill in terms of simulating extreme growths which is not a surprise because the added functionalities are not expected to improve the climate sensitivities of ORCHIDEE (Fig. 9d).

## 5. Discussion



15 The wealth of approaches available for modelling tree ring growth (see the introduction for a summary) has been largely overlooked by the global land-surface community and until now, benchmarking land-surface models against ring-width records still relies mostly on interannual variation in the simulated net primary productivity as a proxy for TRW (Klesse et al., 2018; Kolus et al., 2019; Rammig et al., 2015; Zhang et al., 2018). Although such an approach is valid to benchmark the capability of land-surface models to simulate interannual variability, the observations will need to be detrended to remove the size-related growth signal, adding considerable uncertainty to the benchmark (Bunde et al., 2013; Cedro, 2016; Nicklen et al., 2019; Stine, 2019). Moving beyond the net primary production proxy by explicitly simulating TRW enriches the benchmark since potentially confounding factors including climate responses, forest structure, age and size trends (Alexander et al., 2018; Nickless et al., 2011), as well as sampling biases (Babst et al., 2014a), can be better accounted for. Whereas previous studies had to rely on a single qualitative benchmark, i.e., interannual variability, our method shows that at least four benchmarks, each of them defined by two metrics, are available for models that meet the minimal requirements to simulate TRW determined by Cook's aggregate tree growth model (Fig. 2).

Irrespective of the model approach, the largest archive of tree-ring records that is freely available to the land-surface community, i.e., the ITRDB, is notorious for its sample biases (Klesse et al., 2018; Zhao et al., 2019). Although it may be difficult to correct the data for these biases, we propose two solutions for comparing LSM output to biased observations. Simulating a size-structured population of trees enables comparing the observations relative to a benchmark tall simulated tree, which compensates for the tendency of dendroclimatic samplers to select the oldest trees in a stand (which often turn out to be the larger trees). Although the ITRDB does not contain the site metadata that would be required to make this comparison exact, i.e., the diameter and true age distribution of the sampled stand, it protects against comparing extreme samples to mean simulations. The second solution relies on the observation that the variation due to size-related growth by far exceeds the variation due to environmental changes and helps to constrain the survivor bias which is derived from the growth of young fast-growing trees that died a long time ago and are therefore absent from records made from present day sampling of old growth forests. The benchmarks proposed here provide a tool to start using TRWs as a much-needed large-scale constraint on the maximum tree diameter and annual growth for the transition from pre-industrial to present-day environmental conditions.



40

Combining these two solutions with targeted processes resulted in four benchmarks, each of them defined by two metrics (Table 1). The test case demonstrated that these benchmarks were largely independent in terms of their information content and thus resulted in a rich and rather refined description of the remaining model deficiencies (Fig. 9). The novel benchmarks proposed here provide new targets for evaluating land-surface models' performance as each of the eight metrics could be used in the objective function of any data assimilation technique to rigorously account for the information contained in TRW records.

45

Tree-ring records thus should complement well-established but short-term benchmarks for land-surface models (Randerson et al., 2009), such as forest inventory data (Bellassen et al., 2010; Naudts et al., 2015), FLUXNET sites (Blyth et al., 2010; Williams et al., 2009), Free Air CO<sub>2</sub> Enrichment experiments (De Kauwe et al., 2013) and satellite observations of vegetation activity (Chen et al., 2011; Demarty et al., 2007). The value of tree-ring records can be further enriched by developing new and unbiased networks to complement the ITRDB, adding their stable isotope ratios (Levesque et al., 2019; Barichivich et al. in prep.) and combining their use with high-frequency but short-term eddy covariance measurements (Curtis et al., 2002), experimental data from plant growth under pre-industrial CO<sub>2</sub> concentrations (Temme et al., 2015), and proxies of atmospheric composition (Campbell et al., 2017).

50

55

## 7. Code and data availability

In line with GMD requirements, the model code has been archived and made accessible: <https://doi.org/10.14768/20200228001.1>. The scripts required for reproducing the figures, the ORCHIDEE simulations and intermediate results are available at [https://github.com/j-jeong/J.Jeong\\_GMD\\_2020](https://github.com/j-jeong/J.Jeong_GMD_2020). BACI dataset is freely available in online: <http://www.baci-h202i0.eu> but requires registration by email.

60

## 8. Competing interest

The authors declare that they have no conflict of interest.



.65

## 9. author contribution

Proposed benchmarks are the outcome of discussions between JJ, JB, PP, VH, and SL. JJ ran the model, analysed the output and prepared figures. FB collected and shared BACI data. JJ and SL wrote the first version of the manuscript, all authors contributed to revising and editing the final manuscript.

.70

## 10. Acknowledgements

JJ, PP, MJM and SL were funded by the VERIFY project under the European Union's Horizon 2020 research and innovation programme under grant agreement No. 776810. JB was supported by the Centre National de la Recherche Scientifique (CNRS) of France through the program "Make Our Planet Great Again". VH acknowledges support from the Earth Systems and Climate Change Hub, funded by the Australian Government's National Environmental Science Program. SL would like to thank Antonio Lara for early discussions on the topic. MNE was supported by NSF/AGS1903626 and the University of Maryland, and acknowledges insights arising from work with the PAGES/Data Assimilation and Proxy System Modeling Working Group.

.75

<https://doi.org/10.5194/gmd-2020-29>  
Preprint. Discussion started: 14 April 2020  
© Author(s) 2020. CC BY 4.0 License.



## Table



80 **Table 1.** Characteristics of four benchmarks making use of ITRDB records. These benchmarks were designed to better constrain physiological and ecological processes in land-surface models. Given the use of the ITRDB data, the benchmarks had to propose solutions for well-known issues of the ITRDB (Table S2).

| Benchmark                          | Metrics  | Targeted process understanding   | Solutions for meaningful comparison with ITRDB   | model Figure |
|------------------------------------|--|--|--|--------------|
| Size dependent growth              | <ul style="list-style-type: none"> <li>· RMSE (Fig. 9a X-axis)</li> <li>· Slope of the residuals (Fig. 9a Y-axis)</li> </ul> | <ul style="list-style-type: none"> <li>· Size-related growth</li> <li>· Within-stand competition</li> </ul>                              | <ul style="list-style-type: none"> <li>· Select the biggest tree of the simulation</li> <li>· Construct an average virtual tree aligned by tree age</li> </ul>                 | Fig. 5       |
| Diameter increment of mature trees | <ul style="list-style-type: none"> <li>· RMSE (Fig. 9b X-axis)</li> <li>· Slope of the residuals (Fig. 9b Y-axis)</li> </ul> | <ul style="list-style-type: none"> <li>· Tree growth</li> <li>· Temporal shift in drivers</li> <li>· Within-stand competition</li> </ul> | <ul style="list-style-type: none"> <li>· Select the biggest tree of the simulation</li> <li>· Construct an average virtual tree aligned by calendar year</li> </ul>            | Fig. 6       |
| Diameter increment of young trees  | <ul style="list-style-type: none"> <li>· RMSE (Fig. 9c X-axis)</li> <li>· Slope of the residuals (Fig. 9c Y-axis)</li> </ul> | <ul style="list-style-type: none"> <li>· Tree growth</li> <li>· Temporal shift in drivers</li> <li>· Size-related growth</li> </ul>      | <ul style="list-style-type: none"> <li>· Select the biggest tree of the simulation</li> <li>· Construct a fast-growing virtual tree</li> </ul>                                 | Fig. 7       |
| Extreme growth                     | <ul style="list-style-type: none"> <li>· Extreme events (Fig. 9d X-axis)</li> <li>· Amplitude (Fig. 9d Y-axis)</li> </ul>    | <ul style="list-style-type: none"> <li>· Climate sensitivity</li> </ul>  | <ul style="list-style-type: none"> <li>· Select the biggest tree of the simulation</li> <li>· Define extreme growth using 25% smallest and 75% largest observations</li> </ul> | Fig. 8       |

85



**Table 2.** Description of the processes included in the four configurations used in the test case

| <b>Configuration</b> | <b>Nitrogen dynamics</b> | <b>Recruitment</b> | <b>Refined within-stand competition</b> | <b>Carbon, water and energy cycles</b> |
|----------------------|--------------------------|--------------------|---|--|
| Ndyn                 | +                        | +                  | +                                       | +                                      |
| Recur                | -                        | +                  | +                                       | +                                      |
| Power                | -                        | -                  | +                                       | +                                      |
| Basic                | -                        | -                  | -                                       | +                                      |



490 **Figures**

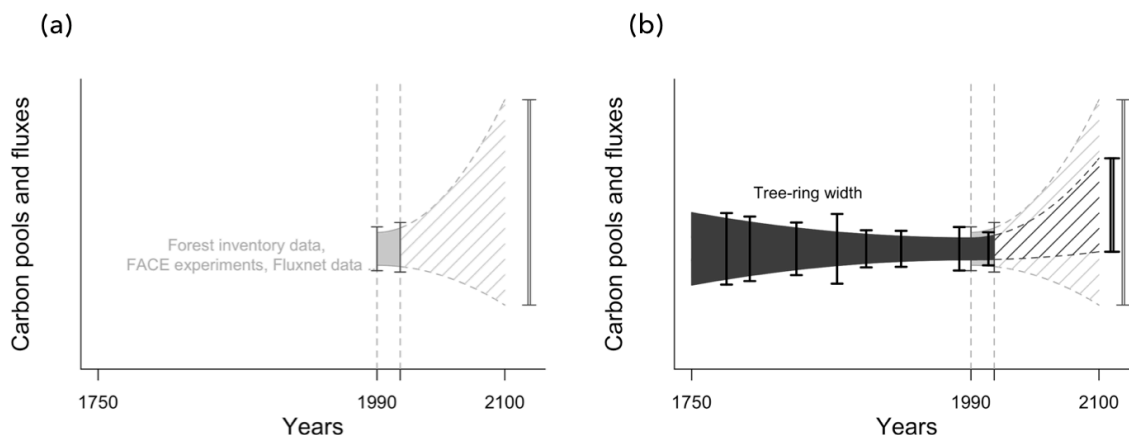


**Figure 1. Conceptual illustration of the expected reduction in model uncertainty following the use of tree-ring width records to benchmark land-surface models.** Note that the anticipated uncertainty reduction assumes that a large part of the model uncertainty comes from the model formulation and its parameters rather than from the initial conditions and drivers. (a) Observational constraints (grey vertical bars) from short-term benchmarks such as forest inventory data, FACE experiments, and FLUXNET data, have been used to parameterize and evaluate the response of ecosystems to environmental changes (light-grey coloured area). When used in projecting the present-day to future carbon pools and fluxes, uncertainty in ecosystem response to climate change is propagated through the model resulting in unacceptably large uncertainties (light-grey hatched area). (b) Tree-ring records going back to pre-industrial times (black vertical bars) are expected to better constrain the response of ecosystems to environmental changes (dark-grey coloured area) which should result in smaller uncertainties when used to project future ecosystem responses (dark-grey hatched area).



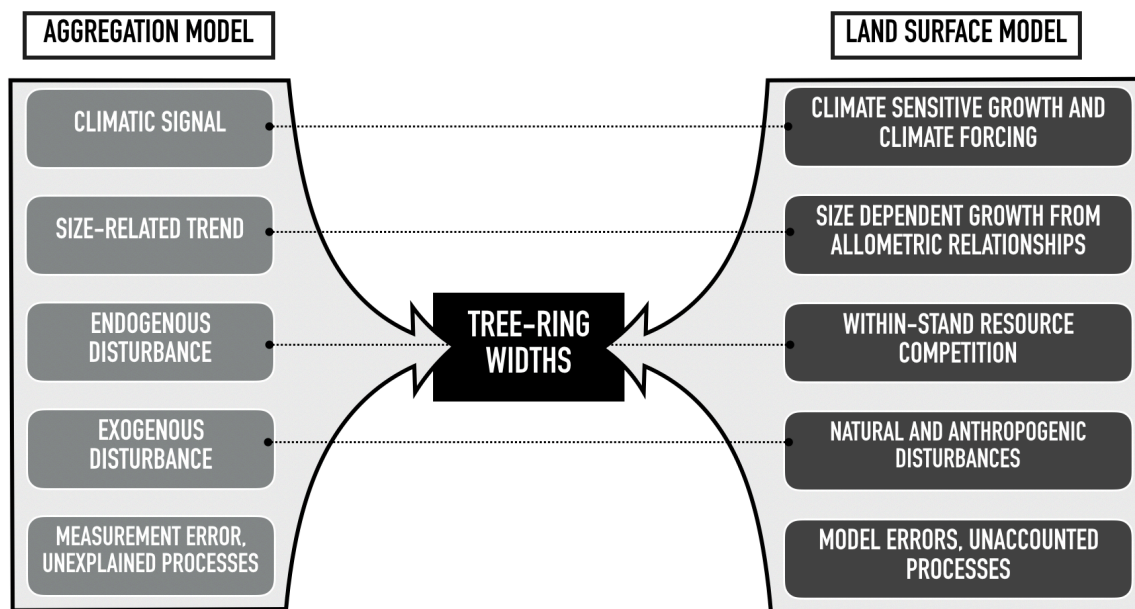


**Figure 2. Main drivers of the aggregate tree growth model of tree-ring growth and the equivalent processes in land-surface models.**

The dotted lines connect the related components. Note that both the aggregation and the land-surface model come with errors, uncertainties

505 and unaccounted processes which are not explicitly modelled.

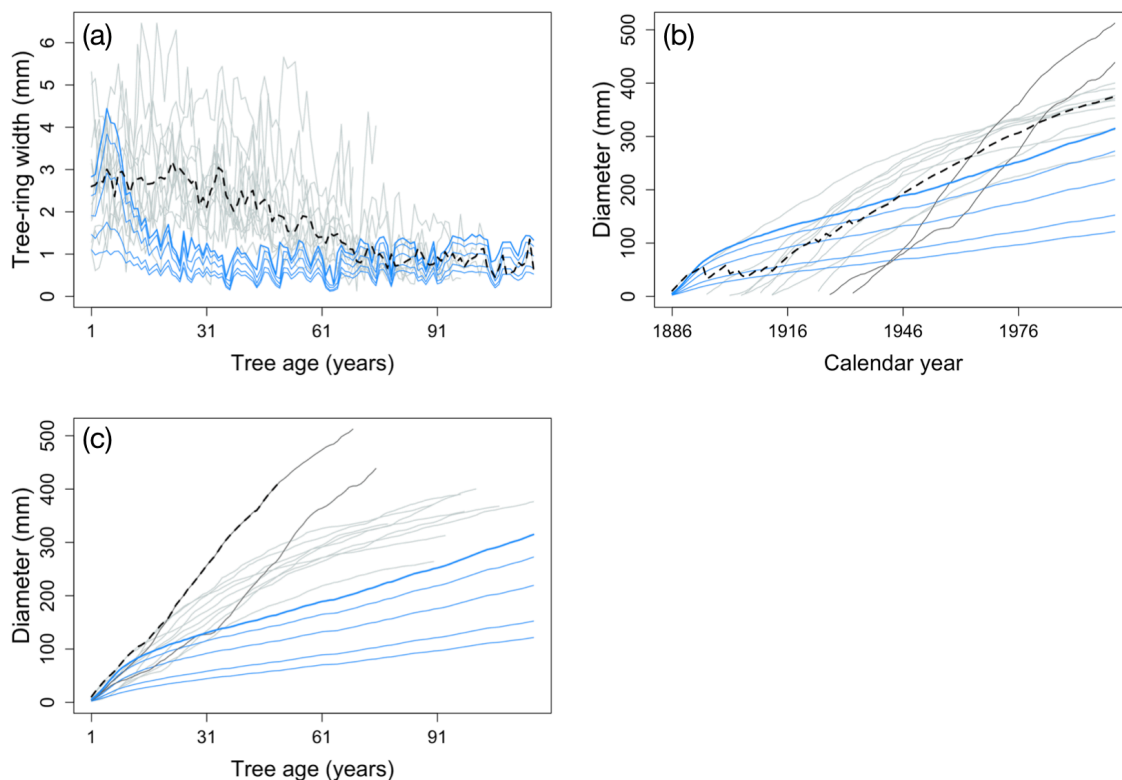


**Figure 3. Solutions and virtual tree compilations to account for challenges to use ITRDB datasets when evaluating land-surface models against ITRDB tree-ring data.** (a) Data-model comparison may overcome the big-tree selection bias by compare only the simulated biggest diameter class (bold blue line) for evaluation rather than all diameter classes (thin blue lines), with compiled virtual tree (black dotted line). Grey lines represent individual trees from observations. (b) The observed tree-ring records are a mixture of relatively slowly-growing trees (light-grey lines) and fast-growing trees (dark-grey lines). Fast-growing trees don't attain the same age as slowly-growing trees because they tend to die earlier. Without further consideration this would lead to underestimating tree growth at the time of stand establishment and thus result in a flawed test when compared against simulated tree growth (blue line) as the virtual tree (black dotted line) much smaller at the establishment. (c) Aligning observations by the age of individual trees better reconstructs tree growth during stand establishment, facilitating data-model comparison. Note the change in the label of the X-axis between panels (b) and (c). Observations taken from a French oak forest archived as germ214 (NOAA, 2020b) (Table S2).

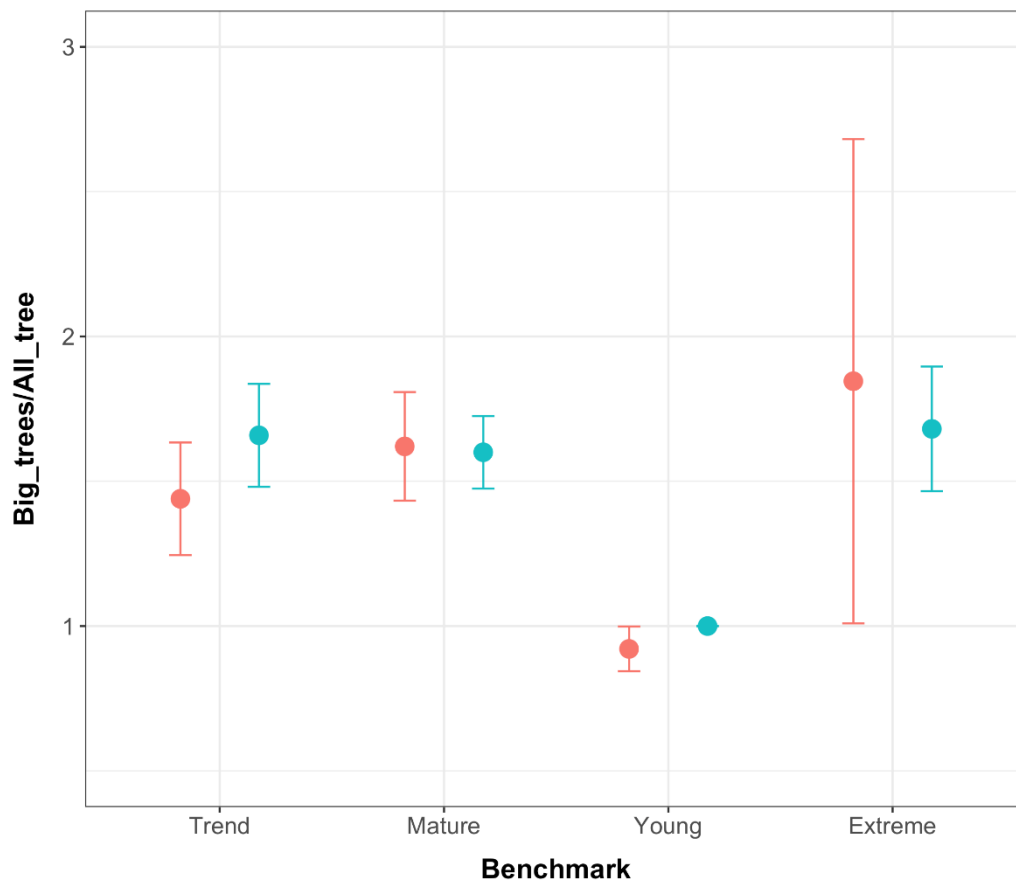


**Figure 4.** Comparison of bias for each of the benchmarks introduced by sampling the 15% biggest trees rather than the average tree (red; observational based) and the bias introduced by reporting the largest simulated diameter class rather than the average tree (blue; model based). Error bars are the standard deviation of the 27 coniferous sites for the BACI data set (red) or the 40 model configurations (4 model different set-ups for 10 sites each).

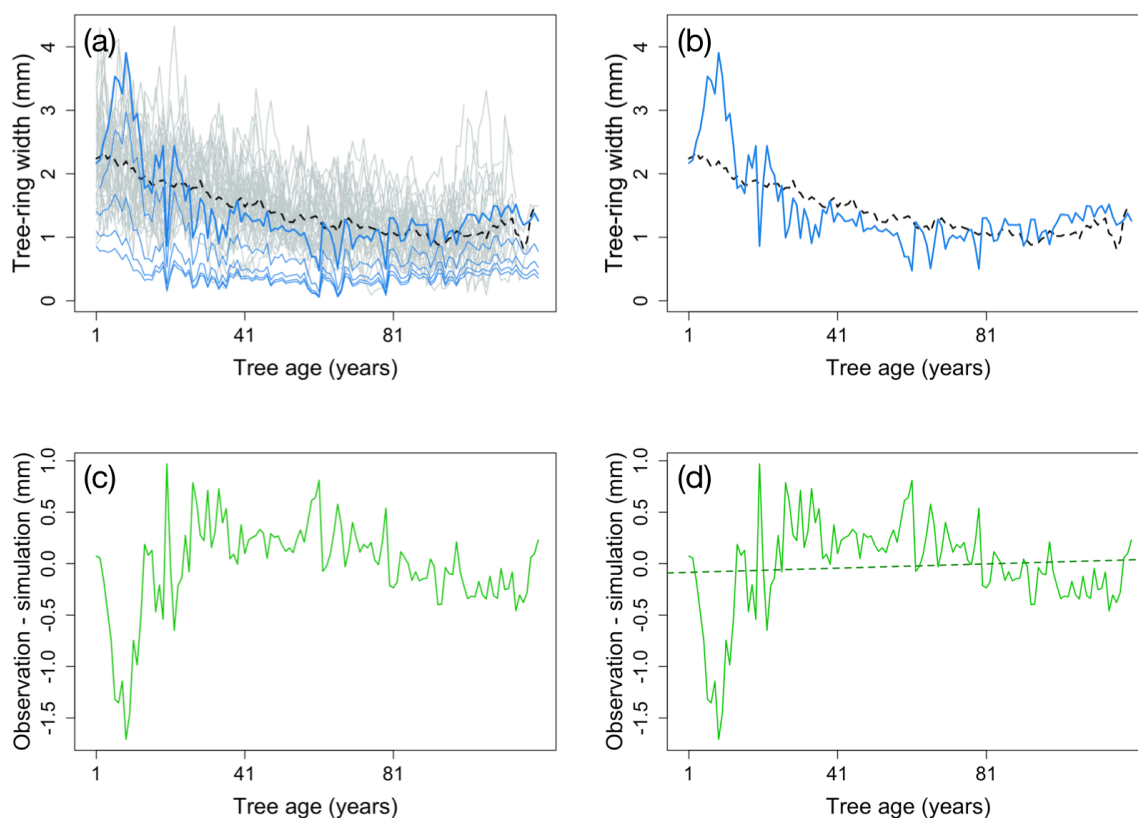


**Figure 5. Illustration of the major steps in calculating the metrics of the benchmark for the size-related trend in diameter increment.**

525 The size-related trend in diameter increment can be assessed by calculating a time series for the average ring width after aligning the age of the individual trees (a, b). Observations are shown as grey lines and simulation as blue lines. The biggest class is presented by the bold line. The black dotted lines represent the virtual tree based on the observations. The TRWs of this virtual tree are then subtracted from the simulated TRWs of the largest diameter class (c). Subsequently, a linear regression is used to quantify the temporal trend in the residuals (d). The green line denotes the model residuals and the green dotted line is the linear regression of the model residuals. Furthermore, the root

530 mean square error (RMSE) between the simulations and observations is calculated (not shown) and normalized by the length of time series to calculate the difference in observed and simulated growth trends. Observations and simulation are from site fin052 (NOAA, 2020a) (Table S2).

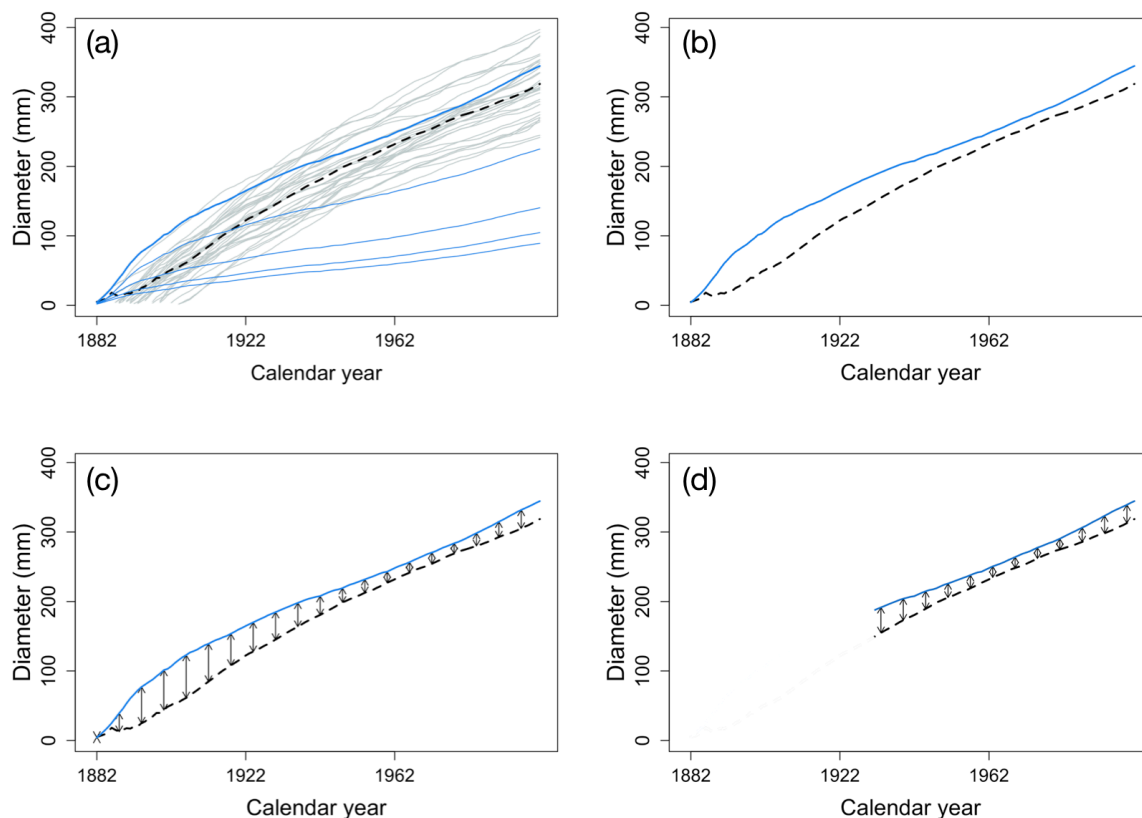


**Figure 6. Illustration of the major steps in calculating the metrics of the benchmark for the diameter increment in mature trees.**

535 Individual tree records are ordered by calendar year and for each year the average observed diameter is calculated (a). Observations are shown as grey lines and simulation as blue lines. The biggest class is presented by the bold line. Black dotted lines represent the yearly average of observations. Note that X-axis in Fig. 6 is different from Fig. 5. Under the assumption that the observed trees are the biggest trees from a given site, the virtual tree is compared with the biggest diameter class from the model (b) and the RMSE is calculated (c). Given that for the most recent decades both the fast and slow growing trees are still alive and could have been sampled, only the recent decades of the  
540 virtual tree growth are compared to the simulations. The RMSE (grey arrows) and trend (not shown) of the residuals between the virtual tree and the largest diameter class simulated are calculated (d). Observations and simulation are from site finl052 (NOAA, 2020a) (Table S2).

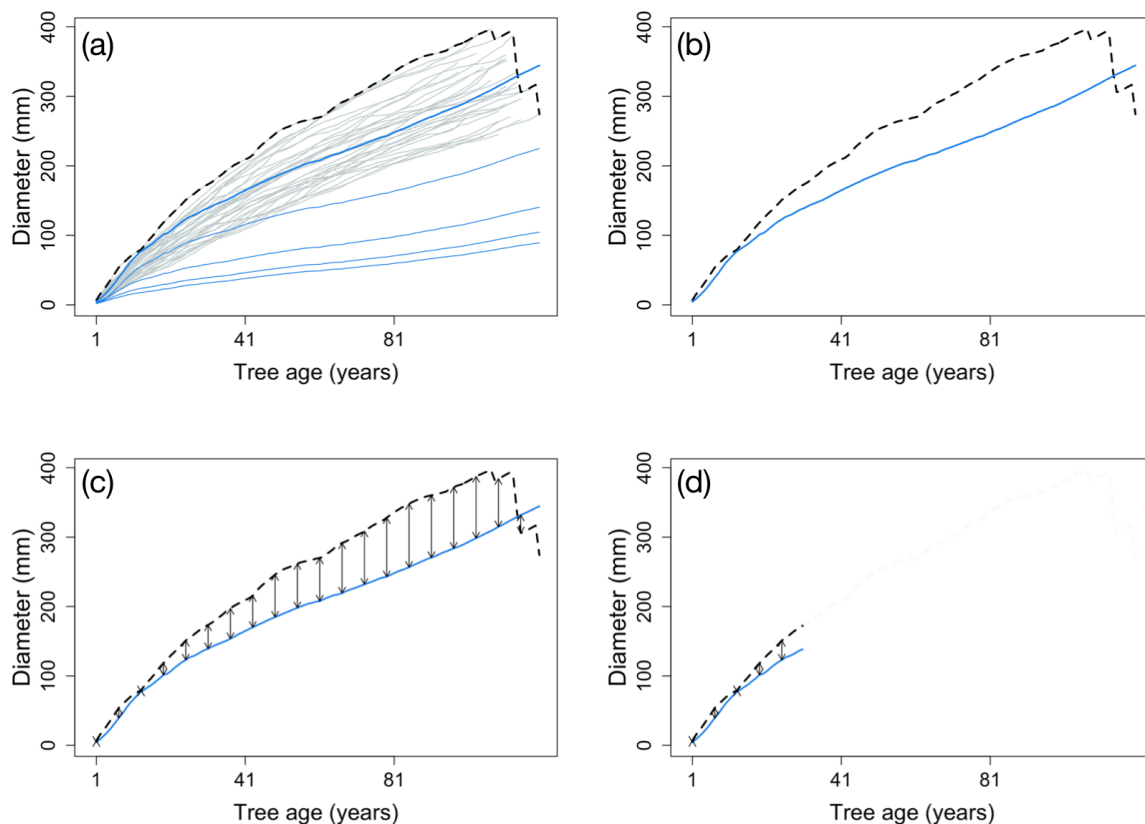


**Figure 7. Illustration of the major steps in calculating the metrics of the benchmark for diameter increment in young trees.** After aligning the TRW records of the individual trees by their age, a virtual tree is constructed by taking the maximum observed diameter of all trees for each year (a). Observations are shown as grey lines and simulation as blue lines. The biggest class is presented by the bold line. Black dotted lines represent the yearly maximum of the observations. The growth of the virtual tree is then compared to the simulated growth of the largest diameter class (b) by calculating the RMSE (c) and trend of the residuals (not shown). These calculations are limited to the first decades of the time series (d) to compensate for the bias caused by the fact that the old fast-growing trees died well before sampling took place. By using different approaches to evaluate the growth of young (this benchmark) and mature trees (the previous benchmark) the comparison accounts for the observation that the drivers of ring growth change when the trees grow taller (Cook, 1985). Observations and simulation are from site finl052 (NOAA, 2020a) (Table S2).

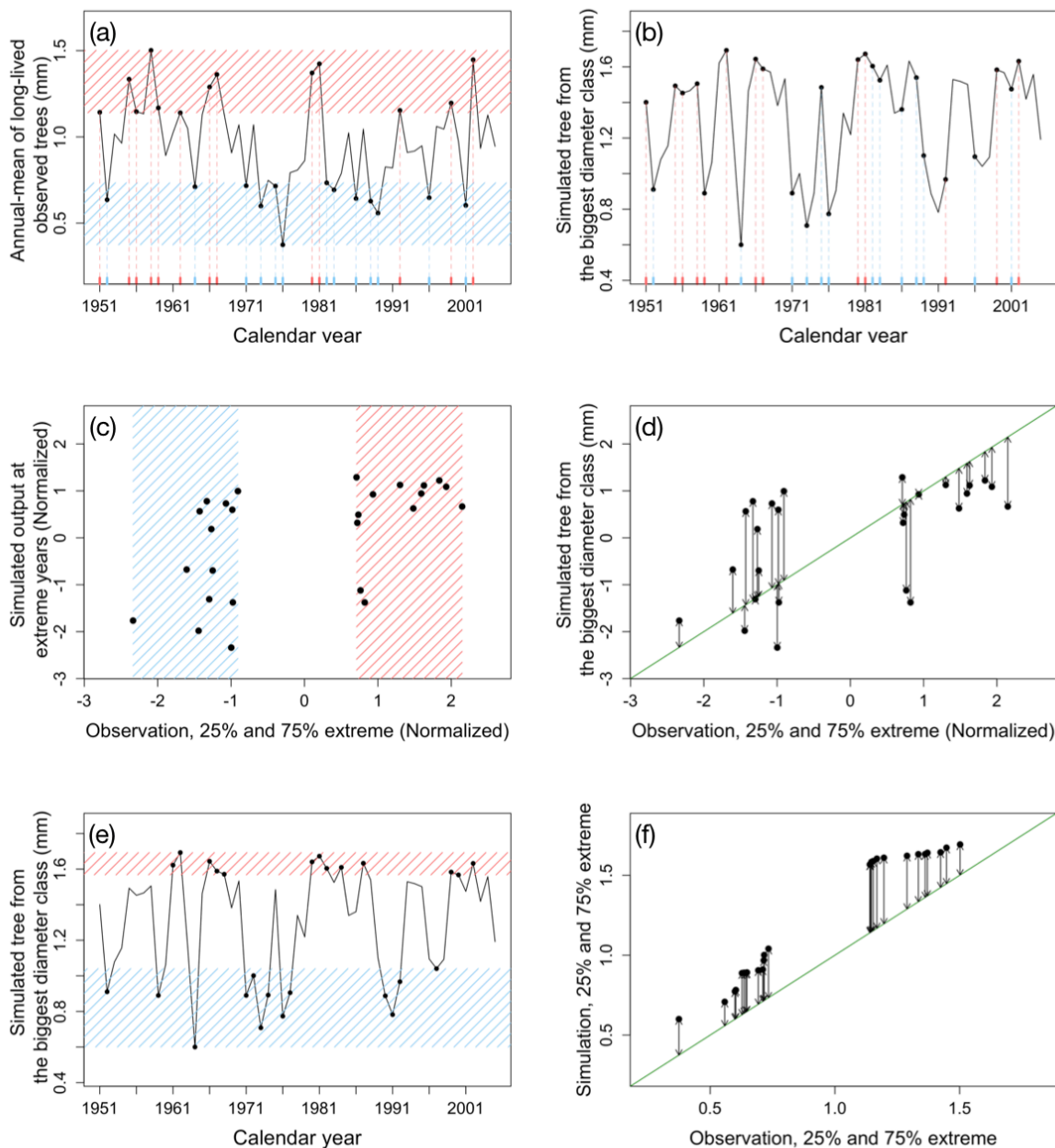


**Figure 8.** Illustration of the major steps in calculating the metrics of the benchmark for extreme growth events. In this benchmark, extreme growth is defined as the first and last quartiles in TRW ordered by calendar year and averaged over the individual trees records (a).

555 Red shaded area and ticks represent observations exceeding the 75 percentile and blue shaded area and ticks represents observation below the 25 percentile (a). The TRW simulated for the largest diameter class are then extracted for the years identified in a (b). Both observations



560 and simulations were normalized to remove the difference in the range of values between configurations. These normalized values correspond to the X and Y axis in (c) and (d) for observation and simulation, respectively. Subsequently, the similarity between simulations and observations was tested by calculating the distance from the 1:1 line (shown in green in d), which is equivalent to the RMSE for years with extreme growth (d). An additional metric is calculated in a similar way but by using both the 25% and 75% extreme values of the simulation and observation regardless of the year (e, f). This test identifies if the simulation can reproduce the amplitude of TRW. To assess the absolute amplitude, the observation and simulation were not normalized. To avoid possible uncertainties from using reconstructed climate forcing, both metrics are limited to the past five decades for which climate observations are available. Observations and simulation are from site spai006 (NOAA, 2020c) (Table S2).

565



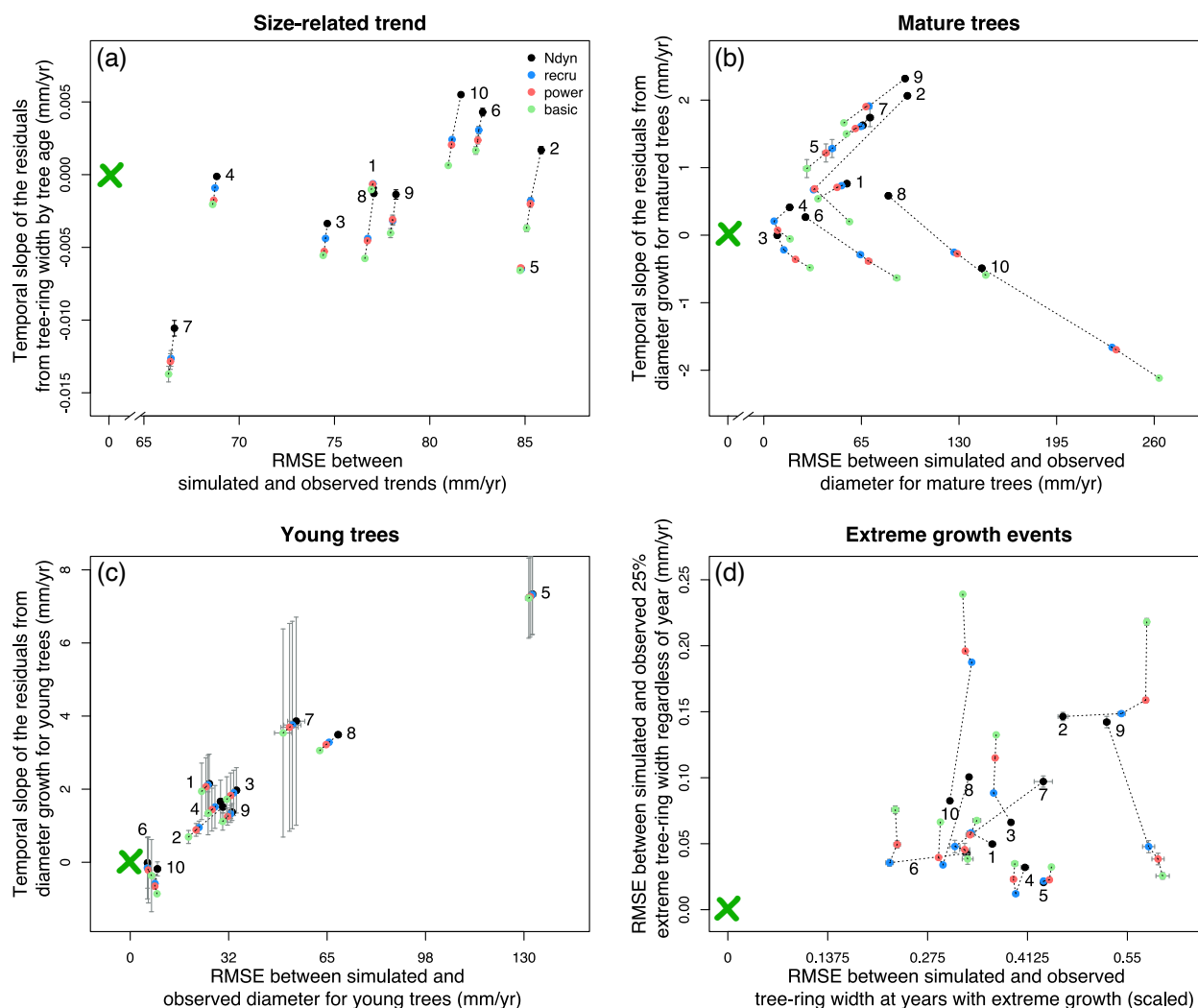


**Figure 9.** The proposed four benchmarks (a-d) applied to a European test case of 10 sites (Table S2 to link numbers to site names and locations). Each colour represents a configuration of the land-surface model (Table 2 details the configurations), where black denotes configuration Ndyn, blue Recru, red Power and green the configuration labelled Basic. The green-X marks indicate the desired outcomes.

570 (a) Benchmark for the trend in tree-ring width. The X-axis shows the RMSE of the difference between simulated and observed trend (Fig. 5b) and the Y-axis shows using the slope of the temporal trend in the residuals (Fig. 5d). (b) Benchmark for diameter increment of mature trees. The X-axis shows the RMSE of the difference between simulation and averaged observation aligned by calendar year for matured trees (Fig. 6d), and the Y-axis shows the slope of the temporal trend in the residuals. (c) Benchmark for diameter increment of young trees. The X-axis shows the differences between simulation and averaged observation aligned by age of trees for young trees (Fig. 7d), and the Y-



575 axis shows the slope of the temporal trend in the residuals. (d) Benchmark for climate sensitivity. The X-axis shows the RMSE of the difference between the observed and simulated tree ring widths for years in which the observed tree ring width was extreme. The Y-axis shows the RMSE of the difference between the observed and simulated extreme tree ring widths irrespective of the year they occur.



## References

- 580 Alexander, M. R., Rollinson, C. R., Babst, F., Trouet, V. and Moore, D. J. P.: Relative influences of multiple sources of uncertainty on cumulative and incremental tree-ring-derived aboveground biomass estimates, *Trees*, 32(1), 265–276, doi:10.1007/s00468-017-1629-0, 2018.
- Amthor, J. S.: The McCree–de Wit–Penning de Vries–Thornley Respiration Paradigms: 30 Years Later, *Ann. Bot.*, 86(1), 1–20, doi:10.1006/anbo.2000.1175, 2000.
- 585 Babst, F., Alexander, M. R., Szejner, P., Bouriaud, O., Klesse, S., Roden, J., Ciais, P., Poulter, B., Frank, D., Moore, D. J. and Trouet, V.: A tree-ring perspective on the terrestrial carbon cycle, *Oecologia*, 176(2), 307–322, doi:10.1007/s00442-014-3031-6, 2014a.
- Babst, F., Bouriaud, O., Alexander, R., Trouet, V. and Frank, D.: Toward consistent measurements of carbon accumulation: A multi-site assessment of biomass and basal area increment across Europe, *Dendrochronologia*, 32(2), 153–161, doi:https://doi.org/10.1016/j.dendro.2014.01.002, 2014b.
- 590 Babst, F., Poulter, B., Bodesheim, P., Mahecha, M. D. and Frank, D. C.: Improved tree-ring archives will support earth-system science, *Nat Ecol Evol*, 1(2), 8, doi:10.1038/s41559-016-0008, 2017.
- Babst, F., Bodesheim, P., Charney, N., Friend, A. D., Girardin, M. P., Klesse, S., Moore, D. J. P., Seftigen, K., Björklund, J. and Bouriaud, O.: When tree rings go global: challenges and opportunities for retro-and prospective insight, *Quat. Sci. Rev.*, 595 197, 1–20, 2018.
- Bakker, J. D.: A new, proportional method for reconstructing historical tree diameters, *Can. J. For. Res.*, 35(10), 2515–2520, doi:10.1139/x05-136, 2005.
- Bellassen, V., Le Maire, G., Dhôte, J. F., Ciais, P. and Viovy, N.: Modelling forest management within a global vegetation model—Part 1: Model structure and general behaviour, *Ecol. Modell.*, 221(20), 2458–2474, doi:10.1016/j.ecolmodel.2010.07.008, 2010.
- 600 Blyth, E., Gash, J., Lloyd, A., Pryor, M., Weedon, G. P. and Shuttleworth, J.: Evaluating the JULES Land Surface Model Energy Fluxes Using FLUXNET Data, *J. Hydrometeorol.*, 11(2), 509–519, doi:10.1175/2009JHM1183.1, 2010.



- Bonan, G. B., Williams, M., Fisher, R. A. and Oleson, K. W.: Modeling stomatal conductance in the earth system: linking leaf water-use efficiency and water transport along the soil–plant–atmosphere continuum, *Geosci. Model Dev.*, 7(5), 2193–2222, doi:10.5194/gmd-7-2193-2014, 2014.
- 605
- Bowman, D. M. J. S., Brienen, R. J. W., Gloor, E., Phillips, O. L. and Prior, L. D.: Detecting trends in tree growth: not so simple, *Trends Plant Sci.*, 18(1), 11–17, doi:10.1016/j.tplants.2012.08.005, 2013.
- Brienen, R. J. W., Gloor, E. and Zuidema, P. A.: Detecting evidence for CO<sub>2</sub> fertilization from tree ring studies: The potential role of sampling biases, *Global Biogeochem. Cycles*, 26(1), n/a-n/a, doi:10.1029/2011GB004143, 2012.
- 610
- Briffa, K. R. and Melvin, T. M.: A Closer Look at Regional Curve Standardization of Tree-Ring Records: Justification of the Need, a Warning of Some Pitfalls, and Suggested Improvements in Its Application, in *Dendroclimatology*, pp. 113–145, Springer., 2011.
- Briffa, K. R., Osborn, T. J. and Schweingruber, F. H.: Large-scale temperature inferences from tree rings: a review, *Glob. Planet. Change*, 40(1), 11–26, doi:https://doi.org/10.1016/S0921-8181(03)00095-X, 2004.
- 615
- Bunde, A., Büntgen, U., Ludescher, J., Luterbacher, J. and von Storch, H.: Is there memory in precipitation?, *Nat. Clim. Chang.*, 3(3), 174–175, doi:10.1038/nclimate1830, 2013.
- Campbell, J. E., Berry, J. A., Seibt, U., Smith, S. J., Montzka, S. A., Launois, T., Belviso, S., Bopp, L. and Laine, M.: Large historical growth in global terrestrial gross primary production, *Nature*, 544(7648), 84–87, doi:10.1038/nature22030, 2017.
- Cao, X., Tian, F., Li, F., Gaillard, M.-J., Rudaya, N., Xu, Q. and Herzschuh, U.: Pollen-based quantitative land-cover reconstruction for northern Asia covering the last 40&thinsp;ka&thinsp;cal&thinsp;BP, *Clim. Past*, 15(4), 1503–1536, doi:10.5194/cp-15-1503-2019, 2019.
- 620
- Cedro, A.: Growth-climate relationships of wild service trees on the easternmost range boundary in Poland, *STR16/04*, 24, doi:10.2312/GFZ.b103-16042, 2016.
- Chen, Y.-Y., Gardiner, B., Pasztor, F., Blennow, K., Ryder, J., Valade, A., Naudts, K., Otto, J., McGrath, M. J., Planque, C. and Luysaert, S.: Simulating damage for wind storms in the land surface model ORCHIDEE-CAN (revision 4262), *Geosci. Model Dev.*, 11(2), 771–791, doi:10.5194/gmd-11-771-2018, 2018.
- 625
- Chen, Y., Yang, K., He, J., Qin, J., Shi, J., Du, J. and He, Q.: Improving land surface temperature modeling for dry land of



- China, J. *Geophys. Res. Atmos.*, 116(D20), doi:10.1029/2011JD015921, 2011.
- Chen, Y., Ryder, J., Bastrikov, V., McGrath, M. J., Naudts, K., Otto, J., Otlé, C., Peylin, P., Polcher, J., Valade, A., Black,  
630 A., Elbers, J. A., Moors, E., Foken, T., van Gorsel, E., Haverd, V., Heinesch, B., Tiedemann, F., Knohl, A., Launiainen, S.,  
Loustau, D., Ogée, J., Vesala, T. and Luysaert, S.: Evaluating the performance of the land surface model ORCHIDEE-CAN  
on water and energy flux estimation with a single- and a multi- layer energy budget scheme, *Geosci. Model Dev. Discuss.*, 1–  
35, doi:10.5194/gmd-2016-26, 2016.
- Compo, G. P., Whitaker, J. S., Sardeshmukh, P. D., Matsui, N., Allan, R. J., Yin, X., Gleason, B. E., Vose, R. S., Rutledge,  
635 G., Bessemoulin, P., Brönnimann, S., Brunet, M., Crouthamel, R. I., Grant, A. N., Groisman, P. Y., Jones, P. D., Kruk, M. C.,  
Kruger, A. C., Marshall, G. J., Maugeri, M., Mok, H. Y., Nordli, Ø., Ross, T. F., Trigo, R. M., Wang, X. L., Woodruff, S. D.  
and Worley, S. J.: The Twentieth Century Reanalysis Project, *Q. J. R. Meteorol. Soc.*, 137(654), 1–28, doi:10.1002/qj.776,  
2011.
- Cook, E. R.: A time series analysis approach to tree ring standardization, 1985.
- 640 Cook, E. R. and Kairiukstis, L. A.: *Methods of Dendrochronology*, edited by E. R. Cook and L. A. Kairiukstis, Springer  
Netherlands, Dordrecht., 1990.
- Cook, E. R., Briffa, K. R., Meko, D. M., Graybill, D. A. and Funkhouser, G.: The “segment length curse” in long tree-ring  
chronology development for palaeoclimatic studies, *The Holocene*, 5(2), 229–237, doi:10.1177/095968369500500211, 1995.
- Curtis, P. S., Hanson, P. J., Bolstad, P., Barford, C., Randolph, J. ., Schmid, H. . and Wilson, K. B.: Biometric and eddy-  
645 covariance based estimates of annual carbon storage in five eastern North American deciduous forests, *Agric. For. Meteorol.*,  
113(1–4), 3–19, doi:10.1016/S0168-1923(02)00099-0, 2002.
- D’Arrigo, R., Wilson, R., Liepert, B. and Cherubini, P.: On the ‘Divergence Problem’ in Northern Forests: A review of the  
tree-ring evidence and possible causes, *Glob. Planet. Change*, 60(3), 289–305,  
doi:https://doi.org/10.1016/j.gloplacha.2007.03.004, 2008.
- 650 Deleuze, C. and Houllier, F.: Simple process-based xylem growth model for describing wood microdensitometric profiles, *J.*  
*Theor. Biol.*, 193(1), 99–113, doi:10.1006/jtbi.1998.0689, 1998.
- Deleuze, C., Pain, O., Dhôte, J.-F. and Hervé, J.-C.: A flexible radial increment model for individual trees in pure even-aged



- stands, *Ann. For. Sci.*, 61(4), 327–335, doi:10.1051/forest:2004026, 2004.
- Demarty, J., Chevallier, F., Friend, A. D., Viovy, N., Piao, S. and Ciais, P.: Assimilation of global MODIS leaf area index  
655 retrievals within a terrestrial biosphere model, *Geophys. Res. Lett.*, 34(15), doi:10.1029/2007GL030014, 2007.
- Drew, D. M., Downes, G. M. and Battaglia, M.: CAMBIUM, a process-based model of daily xylem development in  
Eucalyptus, *J. Theor. Biol.*, 264(2), 395–406, doi:10.1016/j.jtbi.2010.02.013, 2010.
- Ducoudré, N. I., Laval, K. and Perrier, A.: SECHIBA, a New Set of Parameterizations of the Hydrologic Exchanges at the  
Land-Atmosphere Interface within the LMD Atmospheric General Circulation Model, *J. Clim.*, 6(2), 248–273,  
660 doi:10.1175/1520-0442(1993)006<0248:SANSOP>2.0.CO;2, 1993.
- Dufrêne, E., Davi, H., François, C., Le Maire, G., Le Dantec, V. and Granier, A.: Modelling carbon and water cycles in a beech  
forest. Part I: Model description and uncertainty analysis on modelled NEE, *Ecol. Modell.*, 185(2–4), 407–436,  
doi:10.1016/j.ecolmodel.2005.01.004, 2005.
- Farquhar, G. D.: Models of Integrated Photosynthesis of Cells and Leaves, *Philos. Trans. R. Soc. B Biol. Sci.*, 323(1216), 357–  
665 367, doi:10.1098/rstb.1989.0016, 1989.
- Fisher, R. A., Muszala, S., Versteinstein, M., Lawrence, P., Xu, C., McDowell, N. G., Knox, R. G., Koven, C., Holm, J., Rogers,  
B. M., Spessa, A., Lawrence, D. and Bonan, G.: Taking off the training wheels: the properties of a dynamic vegetation model  
without climate envelopes, *CLM4.5(ED)*, *Geosci. Model Dev.*, 8(11), 3593–3619, doi:10.5194/gmd-8-3593-2015, 2015.
- Franklin, O., Johansson, J., Dewar, R. C., Dieckmann, U., McMurtrie, R. E., Brännström, Å. and Dybzinski, R.: Modeling  
670 carbon allocation in trees: a search for principles, *Tree Physiol.*, 32(6), 648–666, doi:10.1093/treephys/tpr138, 2012.
- Friedlingstein, P., Cox, P., Betts, R., Bopp, L., Von Bloh, W., Brovkin, V., Cadule, P., Doney, S., Eby, M., Fung, I., Bala, G.,  
John, J., Jones, C., Joos, F., Kato, T., Kawamiya, M., Knorr, W., Lindsay, K., Matthews, H. D., Raddatz, T., Rayner, P., Reick,  
C., Roeckner, E., Schnitzler, K. G., Schnur, R., Strassmann, K., Weaver, A. J., Yoshikawa, C. and Zeng, N.: Climate-carbon  
cycle feedback analysis: Results from the (CMIP)-M-4 model intercomparison, *J. Clim.*, 19(14), 3337–3353,  
675 doi:10.1175/jcli3800.1, 2006.
- Friedlingstein, P., Meinshausen, M., Arora, V. K., Jones, C. D., Anav, A., Liddicoat, S. K. and Knutti, R.: Uncertainties in  
CMIP5 climate projections due to carbon cycle feedbacks, *J. Clim.*, 27(2), 511–526, doi:10.1175/JCLI-D-12-00579.1, 2014.



- Friend, A. D., Eckes-Shephard, A. H., Fonti, P., Rademacher, T. T., Rathgeber, C. B. K., Richardson, A. D. and Turton, R. H.:  
On the need to consider wood formation processes in global vegetation models and a suggested approach, *Ann. For. Sci.*,  
680 76(2), doi:10.1007/s13595-019-0819-x, 2019.
- Fritts, H. C.: *Tree rings and climate*, Elsevier., 2012.
- Fritts, H. C., Shashkin, A. and Downes, G. M.: A simulation model of conifer ring growth and cell structure, *Tree-ring Anal.*  
*Biol. Methodol. Environ. Asp.* CABI Publ. Wallingford, UK, (January 1999), 3–32, 1999.
- Grissino-Mayer, H. D. and Fritts, H. C.: The International Tree-Ring Data Bank: an enhanced global database serving the  
685 global scientific community, *The Holocene*, 7(2), 235–238, doi:10.1177/095968369700700212, 1997.
- Haverd, V., Smith, B., Cook, G. D., Briggs, P. R., Nieradzick, L., Roxburgh, S. H., Liedloff, A., Meyer, C. P. and Canadell, J.  
G.: A stand-alone tree demography and landscape structure module for Earth system models, *Geophys. Res. Lett.*, 40(19),  
5234–5239, doi:10.1002/grl.50972, 2013.
- Hayat, A., Hackett-Pain, A. J., Pretzsch, H., Rademacher, T. T. and Friend, A. D.: Modeling Tree Growth Taking into Account  
690 Carbon Source and Sink Limitations, *Front. Plant Sci.*, 8, doi:10.3389/fpls.2017.00182, 2017.
- Hecht, A. D. and Tirpak, D.: Framework agreement on climate change: a scientific and policy history, *Clim. Change*, 29(4),  
371–402, doi:10.1007/BF01092424, 1995.
- Hemming, D., Fritts, H., Leavitt, S. W., Wright, W., Long, A. and Shashkin, A.: Modelling tree-ring  $\delta^{13}\text{C}$ , *Dendrochronologia*,  
19(1), 23–38, 2001.
- 695 Hirata, R., Hirano, T., Saigusa, N., Fujinuma, Y., Inukai, K., Kitamori, Y., Takahashi, Y. and Yamamoto, S.: Seasonal and  
interannual variations in carbon dioxide exchange of a temperate larch forest, *Agric. For. Meteorol.*, 147(3), 110–124,  
doi:https://doi.org/10.1016/j.agrformet.2007.07.005, 2007.
- Hölttä, T., Vesala, T., Sevanto, S., Perämäki, M. and Nikinmaa, E.: Modeling xylem and phloem water flows in trees according  
to cohesion theory and Münch hypothesis, *Trees*, 20(1), 67–78, doi:10.1007/s00468-005-0014-6, 2006.
- 700 Hughes, M. K., Swetnam, T. W. and Diaz, H. F.: *Dendroclimatology*, edited by M. K. Hughes, T. W. Swetnam, and H. F.  
Diaz, Springer Netherlands, Dordrecht., 2011.
- IPCC: Annex VI: Expert Reviewers of the IPCC WGI Fifth Assessment Report, in *Climate Change 2013: The Physical Science*



- Basis. Contribution of Working Group I to the Fifth Assessment Report of the Intergovernmental Panel on Climate Change, edited by T. F. Stocker, D. Qin, G.-K. Plattner, M. Tignor, S. K. Allen, J. Boschung, A. Nauels, Y. Xia, V. Bex, and P. M. Midgley, pp. 1497–1522, Cambridge University Press, Cambridge, United Kingdom and New York, NY, USA., 2013.
- 705 Kalnay, E., Kanamitsu, M., Kistler, R., Collins, W., Deaven, D., Gandin, L., Iredell, M., Saha, S., White, G., Woollen, J., Zhu, Y., Leetmaa, A., Reynolds, R., Chelliah, M., Ebisuzaki, W., Higgins, W., Janowiak, J., Mo, K. C., Ropelewski, C., Wang, J., Jenne, R. and Joseph, D.: The NCEP/NCAR 40-Year Reanalysis Project, *Bull. Am. Meteorol. Soc.*, 77(3), 437–471, doi:10.1175/1520-0477(1996)077<0437:TNYRP>2.0.CO;2, 1996.
- 710 De Kauwe, M. G., Medlyn, B. E., Zaehle, S., Walker, A. P., Dietze, M. C., Hickler, T., Jain, A. K., Luo, Y., Parton, W. J., Prentice, I. C., Smith, B., Thornton, P. E., Wang, S., Wang, Y.-P., Wårlind, D., Weng, E., Crous, K. Y., Ellsworth, D. S., Hanson, P. J., Seok Kim, H.-, Warren, J. M., Oren, R. and Norby, R. J.: Forest water use and water use efficiency at elevated CO<sub>2</sub>: a model-data intercomparison at two contrasting temperate forest FACE sites, *Glob. Chang. Biol.*, 19(6), 1759–1779, doi:10.1111/gcb.12164, 2013.
- 715 Keeling, C. D., Chin, J. F. S. and Whorf, T. P.: Increased activity of northern vegetation inferred from atmospheric CO<sub>2</sub> measurements, *Nature*, 382(6587), 146–149, doi:10.1038/382146a0, 1996.
- Klesse, S., Babst, F., Lienert, S., Spahni, R., Joos, F., Bouriaud, O., Carrer, M., Di Filippo, A., Poulter, B., Trotsiuk, V., Wilson, R. and Frank, D. C.: A Combined Tree Ring and Vegetation Model Assessment of European Forest Growth Sensitivity to Interannual Climate Variability, *Global Biogeochem. Cycles*, 32(8), 1226–1240, doi:10.1029/2017GB005856, 2018.
- 720 Kolus, H. R., Huntzinger, D. N., Schwalm, C. R., Fisher, J. B., McKay, N., Fang, Y., Michalak, A. M., Schaefer, K., Wei, Y., Poulter, B., Mao, J., Parazoo, N. C. and Shi, X.: Land carbon models underestimate the severity and duration of drought’s impact on plant productivity, *Sci. Rep.*, 9(1), 2758, doi:10.1038/s41598-019-39373-1, 2019.
- Krinner, G., Viovy, N., de Noblet-Ducoudré, N., Ogée, J., Polcher, J., Friedlingstein, P., Ciais, P., Sitch, S. and Prentice, I. C.: A dynamic global vegetation model for studies of the coupled atmosphere-biosphere system, *Global Biogeochem. Cycles*, 19(1), doi:10.1029/2003GB002199, 2005.
- 725 Laloyaux, P., de Boisseson, E., Balmaseda, M., Bidlot, J.-R., Broennimann, S., Buizza, R., Dalhgren, P., Dee, D., Haimberger, L., Hersbach, H., Kosaka, Y., Martin, M., Poli, P., Rayner, N., Rustemeier, E. and Schepers, D.: CERA-20C: A Coupled





- Reanalysis of the Twentieth Century, *J. Adv. Model. Earth Syst.*, 10(5), 1172–1195, doi:10.1029/2018MS001273, 2018.
- LaMarche, V. C., Graybill, D. A., Fritts, H. C. and ROSE, M. R.: Increasing Atmospheric Carbon Dioxide: Tree Ring Evidence  
730 for Growth Enhancement in Natural Vegetation, *Science* (80-. ), 225(4666), 1019–1021, doi:10.1126/science.225.4666.1019,  
1984.
- Levesque, M., Andreu-Hayles, L., Smith, W. K., Williams, A. P., Hobi, M. L., Allred, B. W. and Pederson, N.: Tree-ring  
isotopes capture interannual vegetation productivity dynamics at the biome scale, *Nat. Commun.*, 10(1), 742,  
doi:10.1038/s41467-019-08634-y, 2019.
- 735 Li, G., Harrison, S. P., Prentice, I. C. and Falster, D.: Simulation of tree-ring widths with a model for primary production,  
carbon allocation, and growth, *Biogeosciences*, 11(23), 6711–6724, doi:10.5194/bg-11-6711-2014, 2014.
- Luo, Y. Q., Randerson, J. T., Friedlingstein, P., Hibbard, K., Hoffman, F., Huntzinger, D., Jones, C. D., Koven, C., Lawrence,  
D., Li, D. J., Abramowitz, G., Bacour, C., Blyth, E., Carvalhais, N., Ciais, P., Dalmonech, D., Fisher, J. B., Fisher, R.,  
Friedlingstein, P., Hibbard, K., Hoffman, F., Huntzinger, D., Jones, C. D., Koven, C., Lawrence, D., Li, D. J., Mahecha, M.,  
740 Niu, S. L., Norby, R., Piao, S. L., Qi, X., Peylin, P., Prentice, I. C., Riley, W., Reichstein, M., Schwalm, C., Wang, Y. P., Xia,  
J. Y., Zaehle, S. and Zhou, X. H.: A framework for benchmarking land models, *Biogeosciences*, 9(10), 3857–3874,  
doi:10.5194/bg-9-3857-2012, 2012.
- Magnani, F., Mencuccini, M., Borghetti, M., Berbigier, P., Berninger, F., Delzon, S., Grelle, A., Hari, P., Jarvis, P. G., Kolari,  
P., Kowalski, A. S., Lankreijer, H., Law, B. E., Lindroth, A., Loustau, D., Manca, G., Moncrieff, J. B., Rayment, M., Tedeschi,  
745 V., Valentini, R. and Grace, J.: The human footprint in the carbon cycle of temperate and boreal forests, *Nature*, 447(7146),  
849–851, doi:10.1038/nature05847, 2007.
- McGuffie A., K. and H.: Practical Climate Modelling, in *A Climate Modelling Primer.*, 2005.
- Melvin, T.: Historical growth rates and changing climatic sensitivity of boreal conifers, *University of East Anglia.*, 2004.
- Mencuccini, M., Martínez-Vilalta, J., Vanderklein, D., Hamid, H. A., Korakaki, E., Lee, S., Michiels, B., Martínez-Vilalta, J.,  
750 Vanderklein, D., Hamid, H. A., Korakaki, E., Lee, S. and Michiels, B.: Size-mediated ageing reduces vigour in trees, *Ecol.*  
*Let.*, 8(11), 1183–1190, doi:10.1111/j.1461-0248.2005.00819.x, 2005.
- Merganičová, K., Merganič, J., Lehtonen, A., Vacchiano, G., Sever, M. Z. O., Augustynczyk, A. L. D., Grote, R., Kyselová,



- I., Mäkelä, A., Yousefpour, R., Krejza, J., Collalti, A. and Reyer, C. P. O.: Forest carbon allocation modelling under climate change, *Tree Physiol.*, doi:10.1093/treephys/tpz105, 2019.
- 755 Misson, L., Rathgeber, C. and Guiot, J.: Dendroecological analysis of climatic effects on *Quercus petraea* and *Pinus halepensis* radial growth using the process-based MAIDEN model, *Can. J. For. Res.*, 34(4), 888–898, doi:10.1139/x03-253, 2004.
- Moorcroft, P. R., Hurtt, G. C. and Pacala, S. W.: A Method for Scaling Vegetation Dynamics: The Ecosystem Demography Model (ED), *Ecol. Monogr.*, 71(4), 557–585, doi:10.2307/3100036, 2001.
- Nash, S. E.: Fundamentals of tree-ring research. James H. Speer., *Geoarchaeology*, 26(3), 453–455, doi:10.1002/gea.20357,  
760 2011.
- Naudts, K., Ryder, J., McGrath, M. J., Otto, J., Chen, Y., Valade, A., Bellasen, V., Berhongaray, G., Bönisch, G., Campioli, M., Ghattas, J., De Groot, T., Haverd, V., Kattge, J., MacBean, N., Maignan, F., Merilä, P., Penuelas, J., Peylin, P., Pinty, B., Pretzsch, H., Schulze, E. D., Solyga, D., Vuichard, N., Yan, Y. and Luyssaert, S.: A vertically discretised canopy description for ORCHIDEE (SVN r2290) and the modifications to the energy, water and carbon fluxes, *Geosci. Model Dev.*, 8(7), 2035–  
765 2065, doi:10.5194/gmd-8-2035-2015, 2015.
- Nehrbass-Ahles, C., Babst, F., Klesse, S., Nötzli, M., Bouriaud, O., Neukom, R., Dobbertin, M. and Frank, D.: The influence of sampling design on tree-ring-based quantification of forest growth, *Glob. Chang. Biol.*, 20(9), 2867–2885, doi:10.1111/gcb.12599, 2014.
- Nicklen, E. F., Roland, C. A., Csank, A. Z., Wilmking, M., Ruess, R. W. and Muldoon, L. A.: Stand basal area and solar  
770 radiation amplify white spruce climate sensitivity in interior Alaska: Evidence from carbon isotopes and tree rings, *Glob. Chang. Biol.*, 25(3), 911–926, doi:10.1111/gcb.14511, 2019.
- Nickless, A., Scholes, R. J. and Archibald, S.: A method for calculating the variance and confidence intervals for tree biomass estimates obtained from allometric equations, *S. Afr. J. Sci.*, 107(5/6), 86–95, doi:10.4102/sajs.v107i5/6.356, 2011.
- NOAA: finl052, NOAA/WDS for Paleoclimatology, <https://www.ncdc.noaa.gov/paleo/study/3998>, 2020a.
- 775 NOAA: germ214, NOAA/WDS for Paleoclimatology, <https://www.ncdc.noaa.gov/paleo/study/16747>, 2020b.
- NOAA: spai006, NOAA/WDS for Paleoclimatology, <https://www.ncdc.noaa.gov/paleo/study/4405>, 2020c.
- Oliver, C. D. and Larson, B. C.: *Forest stand dynamics*, Wiley New York., 1996.



- Ols, C., Girardin, M. P., Hofgaard, A., Bergeron, Y. and Drobyshev, I.: Monitoring Climate Sensitivity Shifts in Tree-Rings of Eastern Boreal North America Using Model-Data Comparison, *Ecosystems*, 21(5), 1042–1057, doi:10.1007/s10021-017-0203-3, 2018.
- Rammig, A., Wiedermann, M., Donges, J. F., Babst, F., Von Bloh, W., Frank, D., Thonicke, K. and Mahecha, M. D.: Coincidences of climate extremes and anomalous vegetation responses: comparing tree ring patterns to simulated productivity, *Biogeosciences*, 12(2), 373–385, doi:10.5194/bg-12-373-2015, 2015.
- Randerson, J. T., Hoffman, F. M., Thorton, P. E., Mahowald, N. M., Lindsay, K., Lee, Y., Nevison, C. D., Doney, S. C., Bonan, G., Stöckli, R., Covey, C., Running, S. W. and Fung, I. Y.: Systematic assessment of terrestrial biogeochemistry in coupled climate-carbon models, *Glob. Chang. Biol.*, 15(10), 2462–2484, doi:10.1111/j.1365-2486.2009.01912.x, 2009.
- Ryder, J., Polcher, J., Peylin, P., Ottlé, C., Chen, Y., van Gorsel, E., Haverd, V., McGrath, M. J., Naudts, K., Otto, J., Valade, A. and Luyssaert, S.: A multi-layer land surface energy budget model for implicit coupling with global atmospheric simulations, *Geosci. Model Dev.*, 9(1), 223–245, doi:10.5194/gmd-9-223-2016, 2016.
- Sato, H., Itoh, A. and Kohyama, T.: SEIB–DGVM: A new Dynamic Global Vegetation Model using a spatially explicit individual-based approach, *Ecol. Modell.*, 200(3–4), 279–307, doi:10.1016/j.ecolmodel.2006.09.006, 2007.
- De Schepper, V. and Steppe, K.: Development and verification of a water and sugar transport model using measured stem diameter variations, *J. Exp. Bot.*, 61(8), 2083–2099, doi:10.1093/jxb/erq018, 2010.
- Schulman, E.: Longevity under Adversity in Conifers, *Science* (80-. ), 119(3091), 396–399 [online] Available from: <http://www.jstor.org/stable/1682970>, 1954.
- Smith, B.: LPJ-GUESS-an ecosystem modelling framework, *Dep. Phys. Geogr. Ecosyst. Anal. INES, Sölvegatan*, 12, 22362, 2001.
- Steppe, K., De Pauw, D. J. W., Lemeur, R. and Vanrolleghem, P. A.: A mathematical model linking tree sap flow dynamics to daily stem diameter fluctuations and radial stem growth, *Tree Physiol.*, 26(3), 257–273, doi:10.1093/treephys/26.3.257, 2006.
- Stine, A. R.: Global demonstration of local Liebig’s law behavior for tree-ring reconstructions of climate, *Paleoceanogr. Paleoclimatology*, 34, doi:https://doi.org/10.1029/2018PA003449, 2019.



- Temme, A. A., Liu, J. C., Cornwell, W. K., Cornelissen, J. H. C. and Aerts, R.: Winners always win: growth of a wide range of plant species from low to future high CO<sub>2</sub>, *Ecol. Evol.*, 5(21), 4949–4961, doi:10.1002/ece3.1687, 2015.
- 805 Vaganov, E. A., Hughes, M. K. and Shashkin, A. V.: Growth dynamics of conifer tree rings: images of past and future environments, edited by M. K. Hughes, T. W. Swetnam, and H. F. Diaz, Springer, New York., 2006.
- Viovy, N.: CRUNCEP data set, 2016.
- Vuichard, N., Messina, P., Luysaert, S., Guenet, B., Zaehle, S., Ghattas, J., Bastrikov, V. and Peylin, P.: Accounting for carbon and nitrogen interactions in the global terrestrial ecosystem model ORCHIDEE (trunk version, rev 4999): multi-scale  
810 evaluation of gross primary production, *Geosci. Model Dev.*, 12(11), 4751–4779, doi:10.5194/gmd-12-4751-2019, 2019.
- Wilkinson, S., Ogée, J. J., Domec, J.-C. C., Rayment, M. and Wingate, L.: Biophysical modelling of intra-ring variations in tracheid features and wood density of *Pinus pinaster* trees exposed to seasonal droughts, *Tree Physiol.*, 35(3), 305–318, doi:10.1093/treephys/tpv010, 2015.
- Williams, M., Richardson, A. D., Reichstein, M., Stoy, P. C., Peylin, P., Verbeeck, H., Carvalhais, N., Jung, M., Hollinger, D.  
815 Y., Kattge, J., Leuning, R., Luo, Y., Tomelleri, E., Trudinger, C. M. and Wang, Y.-P.: Improving land surface models with FLUXNET data, *Biogeosciences*, 6(7), 1341–1359, doi:10.5194/bg-6-1341-2009, 2009.
- Wilson, B. F. and Howard, R. A.: A computer model for cambial activity, *For. Sci.*, 14(1), 77–90, doi:10.1093/forestscience/14.1.77, 1968.
- Wolf, A., Ciais, P., Bellassen, V., Delbart, N., Field, C. B. and Berry, J. A.: Forest biomass allometry in global land surface  
820 models, *Global Biogeochem. Cycles*, 25(3), doi:10.1029/2010GB003917, 2011.
- Yue, C., Ciais, P., Cadule, P., Thonicke, K., Archibald, S., Poulter, B., Hao, W. M., Hantson, S., Mouillot, F., Friedlingstein, P., Maignan, F. and Viovy, N.: Modelling the role of fires in the terrestrial carbon balance by incorporating SPITFIRE into the global vegetation model ORCHIDEE – Part 1: simulating historical global burned area and fire regimes, *Geosci. Model Dev.*, 7(6), 2747–2767, doi:10.5194/gmd-7-2747-2014, 2014.
- 825 Zaehle, S. and Friend, A. D.: Carbon and nitrogen cycle dynamics in the O-CN land surface model: 1. Model description, site-scale evaluation, and sensitivity to parameter estimates, *Global Biogeochem. Cycles*, 24(1), doi:10.1029/2009GB003521, 2010.



- Zhang, Z., Babst, F., Bellassen, V., Frank, D., Launois, T., Tan, K., Ciais, P. and Poulter, B.: Converging Climate Sensitivities of European Forests Between Observed Radial Tree Growth and Vegetation Models, *Ecosystems*, 21(3), 410–425, doi:10.1007/s10021-017-0157-5, 2018.
- 830
- Zhao, S., Pederson, N., D'Orangeville, L., HilleRisLambers, J., Boose, E., Penone, C., Bauer, B., Jiang, Y. and Manzanedo, R. D.: The International Tree-Ring Data Bank (ITRDB) revisited: Data availability and global ecological representativity, *J. Biogeogr.*, 46(2), 355–368, doi:10.1111/jbi.13488, 2019.
- Zuidema, P. A., Vlam, M. and Chien, P. D.: Ages and long-term growth patterns of four threatened Vietnamese tree species, *Trees*, 25(1 LB-Zuidema2011), 29–38, doi:10.1007/s00468-010-0473-2, 2011.
- 835
- Zuidema, P. A., Poulter, B. and Frank, D. C.: A Wood Biology Agenda to Support Global Vegetation Modelling, *Trends Plant Sci.*, 23(11), 1006–1015, doi:10.1016/j.tplants.2018.08.003, 2018.